
A Foundation Model for Instruction-Conditioned In-Context Time Series Tasks

Anish Saha¹ Konstantin Shmakov¹

Abstract

In-context learning (ICL) is an established paradigm in large language models, enabling task adaptation at inference time through contextual examples rather than parameter updates. While several recent time-series foundation models incorporate forms of contextual conditioning or example-based prompting, these approaches typically rely on implicit positional context, retrieval, or task-specific objectives, rather than explicit instruction-conditioned demonstrations. We propose a foundation model for instruction-conditioned in-context time-series tasks, built on a quantile regression variant of a T5 encoder–decoder architecture, in which historical “examples” and “queries” are represented using a structured, prompt-like tokenization scheme with specialized semantic tokens that explicitly distinguish target series, covariates, context, and task-specific future information. A hierarchical Transformer architecture comprising per-example encoding, example-level fusion, and cross-example attention enables the model to condition its decoding behavior on in-context input–output demonstrations, allowing it to infer forecasting strategies and other time-series tasks without task-specific fine-tuning. The model is trained on a large-scale corpus of real and synthetic time series generated via mixup augmentation and controlled multivariate relationship synthesis, and combines supervised forecasting objective with self-supervised instruction-conditioned tasks such as imputation, reconstruction, classification, and source demixing. We show that this multi-task, example-conditioned training encourages the model to learn a distribution over time-series tasks and mappings, improving its ability to adapt to local structure at inference time. Across datasets spanning diverse domains, frequencies, and horizons, the proposed approach consistently outper-

forms strong foundation baselines on both point and probabilistic forecasting benchmarks, including fev-bench, and GIFT-Eval, while also achieving competitive performance on classification and anomaly detection tasks, demonstrating the effectiveness of structured in-context prompting and hierarchical fusion for flexible, instruction-following time-series foundation models.

1. Introduction

Time series modeling underpins decision-making across a wide range of domains, including retail demand forecasting, energy and load planning, financial risk management, transportation, and industrial operations. These applications rely not only on accurate forecasting, but also on related tasks such as anomaly detection (Audibert et al., 2020), regime classification (Fawaz, 2020), imputation (Cao et al., 2018), and scenario analysis (Gneiting & Katzfuss, 2014). Over the past decades, the field has evolved from classical statistical approaches (Box & Jenkins, 1968) to advanced deep learning techniques (Salinas et al., 2020) introducing a number of capable large-scale time-series foundation models (Woo et al., 2024; Das et al., 2024b; Ansari et al., 2024), trained on diverse datasets, that better capture nonlinear dynamics, long-range dependencies, and complex covariate interactions to achieve strong zero-shot forecasting performance across domains and temporal granularities.

In parallel, in-context learning (ICL) has become an established paradigm in large language models, enabling task adaptation at inference time through contextual input–output examples rather than parameter updates. This behavior was first systematically demonstrated in large-scale language models (Brown et al., 2020), and has since been extended through prompting strategies such as few-shot prompting (Brown et al., 2020), instruction tuning (Wei et al., 2021), and chain-of-thought reasoning (Wei et al., 2022), which substantially improve zero-shot and few-shot performance without fine-tuning. Beyond empirical success, recent work has begun to clarify the mechanisms underlying ICL: Garg et al. 2022 show that Transformers trained on sequences of input–label pairs can implement behaviors such as linear predictors, gradient-descent-like updates, and algorithm selection purely through attention, while Min et al. 2022

¹Walmart, Sunnyvale, USA. Correspondence to: Anish Saha <anish.saha@walmart.com>, Konstantin Shmakov <konstantin.shmakov@walmart.com>.

demonstrate that explicitly training on structured demonstration–query episodes substantially improves ICL ability.

In this work, we bring in-context learning using instruction-conditioned demonstrations to time-series modeling. We propose a foundation model for in-context time-series tasks using a structured, prompt-like tokenization scheme (represented by "examples" and "queries") with specialized semantic tokens that explicitly distinguish target series, covariates, historical context, and task-specific future information. We show that this explicit structure is necessary to handle the (i) heterogeneous temporal dynamics, (ii) variable numbers of covariates, and (iii) probabilistic multi-horizon outputs that characterize real-world time-series problems.

Recent time-series foundation models such as TimesFM/TimesFM-2.5 (Das et al., 2024b;a), ICTSP (Lu et al., 2024), Chronos-2 (Ansari et al., 2025), TOTO (Cohen et al., 2025), and TiRex (Auer et al., 2025) have already explored various forms of contextual conditioning, including long historical windows, retrieval of related series, and example-based inputs. However, in these approaches context is used to improve a fixed task, typically forecasting, instead of functioning as explicit input–output demonstrations that define a task mapping at inference time, as in NLP ICL in our proposed work. This distinction offers the promise of recovering many benefits of fine-tuning such as domain adaptation and task specialization purely through inference-time context.

To endow our model with strong in-context learning capability, we train it on a large-scale corpus of real and synthetic time series using a combination of (1) supervised forecasting objectives, and (2) self-supervised tasks, including imputation, reconstruction, classification, anomaly detection, and source de-mixing. This training regime exposes the model to a distribution of time-series tasks and mappings, encouraging it to learn how to adapt behavior based on contextual demonstrations at inference time (Min et al., 2022). While our approach does not employ an explicit meta-learning formulation with inner-loop optimization (Finn et al., 2017), it can be interpreted as an amortized form of meta-learning, in which task adaptation is learned during pretraining and executed through a single forward pass at inference time.

This formulation addresses a common practical scenario: a practitioner may deploy a foundation model trained primarily for forecasting, only to later encounter the need for related tasks such as anomaly detection, regime classification, or domain-specific forecasting behavior. Rather than collecting new labels and fine-tuning the model, our approach allows these requirements to be expressed directly through in-context examples. Empirically, we show that this instruction-conditioned ICL framework yields strong improvements in both point and probabilistic forecasting accuracy across diverse benchmarks, including fev-bench

(Shchur et al., 2025), and GIFT-Eval (Aksu et al., 2024), while also supporting classification and anomaly detection within the same unified architecture. Our main contributions are:

- **Instruction-conditioned in-context learning for time series.** We introduce a principled formulation of instruction-conditioned in-context learning for time-series data, in which tasks are specified through structured input–output demonstrations at inference time rather than through task-specific heads or fine-tuning.
- To enable example-conditioned inference and prevent representation leakage we propose a hierarchical-encoder decoder architecture together with a structured, **prompt-like tokenization scheme** that explicitly encodes semantic roles (targets, covariates, historical context, and task-specific future information).
- **Amortized meta-learning for time-series foundation models.** We introduce a new training paradigm for time-series foundation models that combines forecasting based supervision with other self-supervised tasks to enable the model to adapt to new tasks and domains purely via in-context examples at inference time.
- **Self-supervised tasks for pretraining time-series foundation model.** We design a suite of self-supervised tasks for time-series pretraining including imputation, reconstruction, classification, anomaly detection, and source de-mixing. We also discuss data augmentation strategies and methods to introduce controlled multivariate relationships in time-series.
- We empirically demonstrate the benefits of (i) instruction-conditioned training, (ii) hierarchical fusion, and (iii) amortized meta-learning, through extensive ablations and analyses. The proposed model achieves competitive or superior zero-shot performance on popular point and probabilistic forecasting benchmarks, while also exhibiting competitive performance on classification and anomaly detection tasks using the same architecture and inference procedure.

2. Related Work

In-Context Learning and Meta-Training In-context learning (ICL) enables models to adapt to new tasks at inference time by conditioning on a small number of input–output demonstrations without parameter updates (Brown et al., 2020). This can further be improved through prompt design (Zhao et al., 2021; Holtzman et al., 2021), and explicitly training models on structured demonstration–query episodes. In-Context Time-Series Predictor (Lu et al., 2024) also demonstrates that conditioning Transformer-based models on example series can significantly improve forecasting

Table 1. Comparison of modeling capabilities and in-context learning (ICL) usage in recent time-series foundation models. While several models support multivariate forecasting and covariate information, only our approach enables instruction-conditioned in-context learning through explicit input–output demonstrations, allowing adaptation to multiple time-series tasks at inference time without retraining. ICL context types: M = multivariate series; CL = cross-learning across a group of series; C = covariate series; T = temporal context from the target series only; D = demonstration-based.

Model	Multi-variate Forecasting	Covariates (Past / Known / Cat.)	In-Context Learning Type	Task Adaptation via Demos (Ex. \rightarrow Q.)
Chronos-2	✓	✓	CL, M	✗
TimesFM-2.5	✗	✗	T	✗
TiRex	✗	✗	T	✗
Moirai-2.0	✗	✗	T	✗
TabPFN-TS	✗	✓ (known, categorical)	C	✗
TOTO	✓	✓ (past)	M	✗
(ours)	✓	✓	D, CL, M	✓ (e.g., classification)

performance, highlighting the importance of example selection and contextual information for time-series prediction.

A substantial line of related work focuses on meta-learning (Vilalta & Drissi, 2002; Finn et al., 2017) and multi-task learning (Evgeniou & Pontil, 2004; Ruder, 2017), through self-supervision. Prior studies that train models on a diverse collection of tasks show improved generalization on new tasks in zero-shot settings (Zhong et al., 2021; Mishra et al., 2022; Wei et al., 2021). MetaICL (Min et al., 2022) bridges these perspectives by demonstrating that multi-task meta-training on demonstration–query episodes significantly improves ICL. Our approach adopts a similar training philosophy, extending instruction-conditioned meta-training to time-series data and enabling amortized task adaptation.

From Classical to Foundation Time-Series Models Classical time-series forecasting methods such as ARIMA (Box & Jenkins, 1968), exponential smoothing (Hyndman & Athanasopoulos, 2018) etc., rely on fitting separate models per series. In contrast, global models such as DeepState (Rangapuram et al., 2018), stacked architectures such as N-BEATS (Oreshkin et al., 2019) and N-HITS (Challu et al., 2023), and transformer-based models including TFT (Lim et al., 2021) and PatchTST (Nie, 2022) have become increasingly common. Recent time-series foundation models have scaled these ideas by training large architectures on diverse datasets to achieve strong zero-shot generalization (Ansari et al., 2025; Cohen et al., 2025; Auer et al., 2025). These models show that increased historical context, covariates, and retrieved examples can substantially improve forecasting performance. Patching-based encoders and decoders, as popularized by Nie 2022, are now widely adopted to improve efficiency and capture long-range temporal dependencies; our model similarly employs patch-based representations within a T5-style encoder–decoder backbone.

Contextual Conditioning and Hierarchical Structure in Time Series These benefits of richer context and example selection for forecasting are demonstrated by Das et al. 2024a;

Ansari et al. 2025; Auer et al. 2025. However, context is typically used to improve a fixed task, with task semantics encoded in model parameters or training objectives. In contrast, our work introduces a hierarchical formulation that explicitly encodes structure from individual time series, to groups of examples, to the full in-context input, enabling demonstrations to define task mappings at inference time.

Table 1 provides a summary of the capabilities of our model with those of existing pretrained models.

3. Methodology

3.1. Problem Formulation and ICL Setup

To study the instruction-conditioned in-context learning setup for time-series tasks, we define the following components.

3.1.1. DATA REPRESENTATION AND GRANULARITY

We define the most granular unit in our formulation as a one-dimensional time series

$$x^{(j)} = (x_1^{(j)}, \dots, x_T^{(j)}) \in \mathbb{R}^T,$$

where j indexes a component (e.g., a target series or a covariate). Each component may contain missing values, handled via a binary mask

$$m^{(j)} = (m_1^{(j)}, \dots, m_T^{(j)}), \quad m_t^{(j)} \in \{0, 1\},$$

where $m_t^{(j)} = 1$ indicates that the value is observed.

3.1.2. MULTIVARIATE TIME SERIES AND COVARIATES

A multivariate time series is defined as a collection of one-dimensional components. We denote the set of target time-series as:

$$X = \{x^{(1)}, \dots, x^{(d_x)}\},$$

and the set of corresponding covariate time-series as:

$$Z = \{z^{(1)}, \dots, z^{(d_z)}\},$$

where d_x and d_z denote the number of target and covariate components, respectively. Each $x^{(j)}$ and $z^{(k)}$ is a one-dimensional time series in \mathbb{R}^T with a corresponding mask.

Categorical covariates are embedded into real-valued scalars using ordinal encoding. Each embedded categorical value is then duplicated across time to form a constant one-dimensional covariate series, ensuring structural consistency with dynamic covariates.

3.1.3. EXAMPLES AND QUERIES

An in-context *example* consists of a multivariate time series split into a historical segment and a future segment:

$$\mathcal{E}_i = (X_i^{\text{hist}}, Z_i^{\text{hist}}, X_i^{\text{fut}}, Z_i^{\text{fut}}),$$

where X_i^{hist} and Z_i^{hist} denote target and covariate components over the historical window, and X_i^{fut} and Z_i^{fut} denote the corresponding components over the future window, with all components retaining their corresponding masks.

A *query* has the same structure as an example’s history:

$$\mathcal{Q} = (X_q^{\text{hist}}, Z_q^{\text{hist}}, Z_q^{\text{fut}}),$$

where future covariates Z_q^{fut} are provided when available, but future targets Y_q^{fut} are withheld and must be predicted by the model.

3.1.4. IN-CONTEXT LEARNING INPUT

An in-context learning (ICL) input consists of a set of N examples

$$\mathcal{S} = \{\mathcal{E}_i\}_{i=1}^N,$$

followed by a query \mathcal{Q} . During both training and inference, all examples include both historical and future segments, while the query includes only historical targets and all available covariates.

3.2. Structured Tokenization and Input Construction

We represent each *example/query* using a prompt-like serialization with semantic role tokens that partition targets, covariates, and task-specific outputs while respecting the granularity and heterogeneity of time-series data.

Each example is serialized into a sequence of role-labeled component segments using specialized semantic tokens. Concretely, an example \mathcal{E}_i , containing $d_x^{(i)}$ target compo-

nents and $d_z^{(i)}$ variates, is serialized as $\text{Ser}(\mathcal{E}_i)$

$$\begin{aligned} &= [\text{START}] \bigoplus_{j=1}^{d_x^{(i)}} ([\text{TARGET_SERIES}] \phi(x_{i,\text{hist}}^{(j)}, m_{i,\text{hist}}^{(j)})) \\ &\quad \bigoplus_{k=1}^{d_z^{(i)}} ([\text{EXO G}] \phi(z_{i,\text{hist}}^{(k)}, m_{i,\text{hist}}^{(k)})) \\ &[\text{MID}] \\ &\quad \bigoplus_{j=1}^{d_x^{(i)}} ([\text{TARGET_SERIES}] \phi(x_{i,\text{fut}}^{(j)}, m_{i,\text{fut}}^{(j)})) \\ &\quad \bigoplus_{k=1}^{d_z^{(i)}} ([\text{FUTURE_EXO G}] \phi(z_{i,\text{fut}}^{(k)}, m_{i,\text{fut}}^{(k)})) \\ &[\text{END}], \end{aligned}$$

where \oplus denotes concatenation, and ϕ is the embedding function $\phi : \mathbb{R}^T \rightarrow \mathbb{R}^{P \times D}$ (where T is time-series length, P is number of patches, and D is embedding dimension) performing normalization, patching, mask concatenation.

The query is serialized similarly, except that future target segments and $[\text{END}]$ are omitted. $\text{Ser}(\mathcal{Q})$

$$\begin{aligned} &= [\text{START}] \bigoplus_{j=1}^{d_x^{(q)}} ([\text{TARGET_SERIES}] \phi(x_{q,\text{hist}}^{(j)}, m_{q,\text{hist}}^{(j)})) \\ &\quad \bigoplus_{k=1}^{d_z^{(q)}} ([\text{EXO G}] \phi(z_{q,\text{hist}}^{(k)}, m_{q,\text{hist}}^{(k)})) \\ &[\text{MID}] \\ &\quad \bigoplus_{k=1}^{d_z^{(q)}} ([\text{FUTURE_EXO G}] \phi(z_{q,\text{fut}}^{(k)}, m_{q,\text{fut}}^{(k)})). \end{aligned}$$

This is done instead of raw concatenation of numeric sequences across multiple series and roles (*target vs covariate vs example vs query*) to prevent representation leakage where attention can mix unrelated subsequences, and the model has no reliable boundary cues. Explicit role and boundary tokens provide discrete anchors so the model can (i) build per-example representations, (ii) align ”inputs” with ”outputs” within each example, and (iii) condition the query’s decoding on demonstrated mappings.

3.2.1. TARGET AND COVARIATE TYPES

We support targets and covariates in five common regimes:

- Univariate target: when $d_x = 1$.
- Multivariate targets: when $d_x > 1$.

- Past-only covariates: available over the historical window, i.e., $d_z^{\text{hist}} \geq 1$ and $d_z^{\text{fut}} = 0$.
- Known covariates: available over history and forecast horizon (e.g., calendar, price plan), i.e., $d_z^{\text{hist}}, d_z^{\text{fut}} \geq 1$.
- No covariates: when $d_z = 0$.

3.2.2. STRUCTURED IN-CONTEXT LEARNING INPUT

An in-context learning (ICL) prompt is formed by concatenating a set of serialized N examples followed by the query:

$$\mathcal{P} = \text{Ser}(\mathcal{E}_1) \oplus \dots \oplus \text{Ser}(\mathcal{E}_N) \oplus \text{Ser}(\mathcal{Q}).$$

The model predicts relevant target time-series (Y_q^{fut}):

$$\hat{Y}_q^{\text{fut}} \equiv \{\hat{x}_{q,\text{fut}}^{(j)}\}_{j=1}^{d_x^{(q)}}.$$

3.3. Amortized Meta-Learning Task Definition

The task is implicitly defined by the structure and semantics of the future target components $\{X_i^{\text{fut}}\}_{i=1}^N$ appearing in the examples. The model is trained to learn a conditional predictor $f_\theta : (\mathcal{P}) \mapsto \hat{Y}_q^{\text{fut}}$, such that:

$$f_\theta(\text{Ser}(\mathcal{Q}) \mid \{\text{Ser}(\mathcal{E}_i)\}_{i=1}^N) \approx \{x_{q,\text{fut}}^{(j)}\}_{j=1}^{d_x^{(q)}},$$

without parameter updates. Different tasks correspond to different interpretations of Y_q^{fut} :

- **Forecasting:** Y_q^{fut} is the future continuation of the target series X_q^{hist} .
- **Imputation / reconstruction:** Y_q^{fut} is the completed version of a masked target X_q^{hist} .
- **Anomaly detection:** Y_q^{fut} is a corrected or denoised target series X_q^{hist} .
- **Classification:** Y_q^{fut} is a constant time series representing a class label for X_q^{hist} , derived from one of the classes present in $\{X_i^{\text{fut}}\}_{i=1}^N$.
- **Source de-mixing:** Y_q^{fut} is a residual or component series derived from the mixture in X_q^{hist} .

Table 2 draws an analogy between self-supervised objectives in NLP and corresponding time-series meta-learning tasks.

During inference, ICL is defined as task adaptation without updating θ . All adaptation is achieved solely by conditioning on the example set $\mathcal{S} = \{\mathcal{E}_i\}_{i=1}^N$ provided in the model’s context window.

Table 2. Analogy between self-supervised objectives in NLP and time-series tasks used for instruction-conditioned training.

NLP Objective	Time-Series Task
Next-token prediction	Forecasting
Masked-span prediction	Imputation
Denosing	Anomaly detection
Classification	Property / regime prediction
Unshuffling	Source de-mixing

3.4. Model Architecture

To enable this example-conditioned inference and prevent representation leakage we propose a hierarchical-encoder decoder architecture. In this section we study its building principles consisting of three components: (i) a shared base time-series encoder ϕ , (ii) hierarchical attention fusion across time series and examples, and (iii) a task-agnostic probabilistic decoder.

3.4.1. BASE TIME-SERIES ENCODER ϕ

All one-dimensional time-series components including target series, covariates, and their corresponding masks are processed by a shared base encoder ϕ . Weight sharing ensures a unified representation space across components, while semantic role information is provided explicitly via structured tokenization.

Given a one-dimensional time series $x^{(j)} \in \mathbb{R}^T$, we reduce scale variability across domains and improves generalization by applying instance-wise z-score normalization (Kim et al., 2021): $\tilde{x}^{(j)} = \frac{x^{(j)} - \mu^{(j)}}{\sigma^{(j)} + \epsilon}$, where $\mu^{(j)}$ and $\sigma^{(j)}$ are computed per component using the history only.

As consistent with recent literature, we use patching (Ansari et al., 2025; Woo et al., 2024; Nie, 2022; Dosovitskiy, 2020). The normalized series is divided into P non-overlapping patches of length p , $\tilde{x}^{(j)} \rightarrow \{\tilde{x}_{(1)}^{(j)}, \dots, \tilde{x}_{(P)}^{(j)}\}$ where, $P = \lceil T/p \rceil$. Masks are patched identically and optionally concatenated as additional channels $\tilde{x}^{(j)} \parallel \tilde{m}^{(j)}$.

Each patch is embedded using a residual block, mapping $\mathbb{R}^{2p \rightarrow D}$, with ReLU, instance-norm and dropout:

$$h_k^{(j)} = \text{FFN}(\tilde{x}_{(k)}^{(j)}) + \tilde{x}_{(k)}^{(j)}, \quad h_k^{(j)} \in \mathbb{R}^D.$$

Stacking over patches yields the encoded representation $\phi(x^{(j)}) \in \mathbb{R}^{P \times D}$.

Note that we do not introduce any absolute timestep-level positional embeddings. However, the T5 maintains relative position embeddings used in the self-attention layers which we retain. Additionally, work done by Das et al. 2024a;b on TimesFM and its variants (based on Haviv et al. 2022) and other leading models (Ansari et al., 2024; Hoo et al., 2025) show that temporal order is preserved implicitly through

patch ordering and self-attention due to the presence of causal attention which encodes positional information when there are more than one stacked transformer layers. This design also improves robustness to variable sequence lengths, heterogeneous temporal granularity across examples, and irregular observation patterns.

3.4.2. HIERARCHICAL ATTENTION FUSION

To learn temporal and variate dependencies, the sequences of tokens are processed by multiple stacked Transformer layers, specifically the T5 encoder (Raffel et al., 2020; Ansari et al., 2025). However, applying self-attention over all patches from all series and examples is computationally inefficient and prone to representation entanglement. We therefore adopt a three-stage hierarchical attention scheme. In the representations below we drop the layer and attention head indices, and scaling factor for brevity.

Stage 1: Individual time-series encoding. Each patched series embedding $\phi(x^{(j)})$ is processed by a shared self-attention stacked T5-encoder:

$$H^{(j)} = \text{Enc}_{\text{ts}}(\phi(x^{(j)})), \quad H^{(j)} \in \mathbb{R}^{P \times D}.$$

This stage captures intra-series temporal dependencies while remaining agnostic to semantic role.

Stage 2: Per-example fusion encoding. For each example \mathcal{E}_i (or the query), encoded target and covariate series $\{H^{(j)}\}$ are serialized along the patch dimension together with learned semantic role token embeddings ([START], [TARGET_SERIES], [EXOQ]), yielding the serialized representation discussed in section 3.2, to get: $S_i \equiv \text{Ser}(\mathcal{E}_i)$, and $S_q \equiv \text{Ser}(\mathcal{Q})$, where, $S_i \in \mathbb{R}^{P_i \times D}$, $S_q \in \mathbb{R}^{P_q \times D}$

The example(s) and query sequence then is encoded using a shared self-attention T5-encoder:

$$\tilde{S}_i = \text{Enc}_{\text{ex}}(S_i) \in \mathbb{R}^{P_i \times D}; \quad \tilde{S}_q = \text{Enc}_{\text{ex}}(S_q) \in \mathbb{R}^{P_q \times D}$$

This stage enables interactions between targets and covariates within an example, while preserving example boundaries via the semantic tokens.

Stage 3: Cross-example fusion via ICL rule extraction.

To aggregate information across examples, we apply pooling and fusion operations.

Example Patch pooling. Each encoded example \tilde{S}_i is summarized along patch dimension using mean pooling:

$$e_i = \frac{1}{P_i} \sum_{k=1}^{P_i} \tilde{S}_{i,k} \in \mathbb{R}^D.$$

Example pooling (ICL rule extractor). The pooled example

representations are then aggregated across N examples:

$$r_q = \frac{1}{N} \sum_{i=1}^N e_i \in \mathbb{R}^D,$$

yielding a global ICL rule representation for the query q .

Query conditioning. The rule embedding r_q is concatenated with the query representation \tilde{S}_q and processed by a cross-example self-attention T5-encoder followed by the rule embedding as a residual connection to stabilize training:

$$\hat{S}_q = \text{Enc}_{\text{icl}}([\tilde{S}_q \parallel r_q]) \in \mathbb{R}^{(P_q+1) \times D}$$

$$\hat{S}_q \leftarrow \hat{S}_q + r_q \in \mathbb{R}^{(P_q+1) \times D}$$

Why hierarchy and mean pooling? Hierarchical fusion preserves semantic boundaries, improves scalability with respect to the number of targets, variates and examples, and stabilizes example-conditioned learning. Additionally, mean pooling is permutation-invariant, parameter-free, and robust to variable numbers of patches and examples, avoiding overfitting to specific example positions.

3.4.3. PROBABILISTIC DECODER

The decoder maps the hierarchy-encoded query representation $\hat{S}_q \in \mathbb{R}^{P_q \times D}$ to task outputs using a direct, non-autoregressive formulation to predict the full forecast horizon in a single forward pass.

Mixture-of-experts cross-attention. Let E denote the number of experts. We introduce a learned expert embedding matrix $E_{\text{moe}} \in \mathbb{R}^{E \times D}$, which serves as a set of expert queries. The decoder performs cross-attention with Query = E_{moe} , Key = \hat{S}_q , Value = \hat{S}_q , yielding expert-conditioned hidden states: $H_{\text{moe}}^{(q)} \in \mathbb{R}^{E \times D}$.

Gating and expert aggregation. A gating network maps the expert hidden states to an aggregated representation:

$$\alpha = \text{softmax}(\text{MLP}(H_{\text{moe}})) \in \mathbb{R}^E,$$

$$h = \sum_{e=1}^E \alpha_e H_{\text{moe}}^{(e)} \in \mathbb{R}^D.$$

Output projection block. The aggregated representation is passed through a residual output block followed by a projection head that directly produces multi-horizon quantile forecasts: $\hat{Y}_q^{\text{fut}} = \text{FFN}_{\text{out}}(h) \in \mathbb{R}^{|Q| \times H}$, where $|Q|$ is the number of quantiles and H is the forecast horizon.

Direct multi-horizon prediction. The decoder predicts the entire forecast horizon jointly, rather than using autoregressive rollouts. This improves inference efficiency and

Table 3. Illustrative distribution of heterogeneous prompt structures used during training. Prompts vary in target dimensionality (d_x), covariate dimensionality (d_z), and number of in-context examples N , exposing the model to diverse structural configurations.

Prompt Structure	d_x	d_z	Example Count (N)
Univariate target, no covariates	1	0	1-4
Multivariate targets, no covariates	2-5	0	1-6
Univariate target, past-only covariates	1	1-3	2-6
Multivariate targets, past-only covariates	2-6	1-4	2-8
Multivariate targets, known covariates	2-8	1-6	3-10

mitigates error accumulation, which is essential for long-horizon forecasting. Prior work has shown that direct multi-step prediction yields better accuracy than autoregressive decoding in time-series settings (Zeng et al., 2023).

Quantile regression loss. The model is trained using the pinball loss configured to predict $|Q| = 9$ distinct quantile levels, equidistantly spaced from 0.1 to 0.9 ($Q = \{0.1, 0.2, \dots, 0.9\}$):

$$\mathcal{L}_{\text{QR}} = \frac{1}{|Q|H} \sum_{p \in Q} \sum_{t=1}^H \ell_p(y_t, \hat{y}_t^{(p)}), \text{ where}$$

$$\ell_p(y, \hat{y}) = \max(p(y - \hat{y}), (p - 1)(y - \hat{y})).$$

Here, ground-truth $y \in \{x_{q,\text{fut}}^{(j)}\}_{j=1}^{d_x^{(q)}}$, and ICL prediction $\hat{y} \in \{\hat{x}_{q,\text{fut}}^{(j)}\}_{j=1}^{d_x^{(q)}}$ for a query q containing $d_x^{(q)}$ targets.

Task-agnostic decoding. The decoder architecture is shared across all tasks. Task semantics are determined entirely by the example futures in the in-context prompt, enabling zero-shot task adaptation without task-specific heads.

Flexibility. This architecture supports variable numbers of targets and covariates, heterogeneous example structures, and mixed task types within a single prompt. All flexibility is handled structurally through tokenization and hierarchical fusion rather than task-specific parameters.

4. Training

4.1. Training

We train the proposed model using instruction-conditioned in-context learning prompts that expose the model to **heterogeneous time-series structures** (section 4.2) and distinct **task classes** (section 4.4). Training is designed to encourage the model to learn a conditional predictor $f_\theta : (\mathcal{P}) \mapsto \hat{Y}_q^{\text{fut}}$ that adapts itself based on contextual demonstrations (ICL prompts \mathcal{P}), without parameter updates at inference time.

4.2. Heterogeneous Prompt Construction

During training, each batch consists of a collection of in-context learning prompts \mathcal{P} with many structures character-

Algorithm 1 Amortized Meta-Learning via Instruction-Conditioned Training

Input: Task distribution \mathcal{T} ; example count N ; model f_θ ; serialization function $\text{Ser}(\cdot)$

Output: Trained parameters θ

while not converged **do**

 Sample a meta-training task $\tau \sim \mathcal{T}$ (Section 4.4)

 Sample N example demonstrations $\{\mathcal{E}_i\}_{i=1}^N$ from task domain τ

$\mathcal{E}_i = (X_i^{\text{hist}}, Z_i^{\text{hist}}, X_i^{\text{fut}}, Z_i^{\text{fut}})$

 Sample a query instance

$\mathcal{Q} = (X_q^{\text{hist}}, Z_q^{\text{hist}}, Z_q^{\text{fut}})$

 Withhold query targets Y_q^{fut}

 Construct the in-context prompt:

$\mathcal{P} = \text{Ser}(\mathcal{E}_1) \oplus \dots \oplus \text{Ser}(\mathcal{E}_N) \oplus \text{Ser}(\mathcal{Q})$

 Predict query output $\hat{Y}_q^{\text{fut}} = f_\theta(\mathcal{P})$

 Compute loss $\mathcal{L}(\hat{Y}_q^{\text{fut}}, Y_q^{\text{fut}})$

 Update parameters $\theta \leftarrow \theta - \eta \nabla_\theta \mathcal{L}$

end while

ized by: (i) the number of target dimensions d_x , (ii) the number of covariates d_z , and (iii) the semantic role of each component ([TARGET_SERIES], [EXOG], [FUTURE_EXOG]).

We include prompts corresponding to: univariate targets ($d_x = 1$), multivariate targets ($d_x > 1$), multivariate targets with past-only covariates, multivariate targets with known future covariates, no covariates ($d_z = 0$). Table 3 summarizes some of the common structures observed.

The structure of the example demonstrations may match or differ from the query structure, depending on the task. This exposes the model to varying degrees of structural alignment between examples and queries, improving robustness to real-world heterogeneity.

4.3. Amortized Meta-Learning via Instruction-Conditioned Training

The model learns a conditional predictor $f_\theta : \mathcal{P} \mapsto \hat{Y}_q^{\text{fut}}$, where the in-context prompt \mathcal{P} defines both the task and the data distribution. Training proceeds by sampling prompts from a distribution over tasks and structures, meta-training the model to perform task adaptation through context.

Algorithm 4.3 summarizes the proposed training procedure. The model is meta-trained across a distribution of time-series tasks and structures. Task adaptation is learned during training and executed at inference time via a single forward pass conditioned on in-context demonstrations.

The model is trained to minimize the expected loss:

$$\min_{\theta} \mathbb{E}_{\mathcal{P} \sim p(\mathcal{P})} [\mathcal{L}(f_\theta(\mathcal{P}), Y_q^{\text{fut}})]$$

where $\mathcal{L}(\cdot, \cdot)$ is the quantile regression loss (section 3.4.3).

Table 4. Implementation mapping of example and query components for different meta-training tasks. Each task is instantiated using the same instruction-conditioned example–query format, with task semantics defined by the example futures. All tasks also include the covariate variables Z_i^{hist} , Z_i^{fut} , Z_q^{hist} , Z_q^{fut} unless specified.

Task	Example History	Example Future	Query History	Model Output	Meta-Training	Inference Adaptation
Forecasting	$X_{i,t:t+L}^{\text{hist}}$	$X_{i,t+L:t+L+H}^{\text{fut}}$	X_q^{hist}	\hat{Y}_q^{fut}	✓	✓
Imputation / Recon.	$\tilde{X}_i^{\text{hist}}$ (masked)	X_i^{hist} (clean)	$\tilde{X}_q^{\text{hist}}$ (missing)	\hat{X}_q^{hist} (reconstructed)	✓	✗
Anomaly Detection	$X_{i,\text{corr}}^{\text{hist}}$	$X_{i,\text{clean}}^{\text{hist}}$	$X_{q,\text{corr}}^{\text{hist}}$	$\hat{X}_{q,\text{clean}}^{\text{hist}}$	✓	✓ ($\hat{Y}_{q,\text{clean}}^{\text{fut}}$)
Classification*	X_i^{hist}	$c_i \cdot \mathbf{1}$	X_q^{hist}	$\hat{c}_i \cdot \mathbf{1}$	✓	✓
Source De-mixing**	$\tilde{X}_i^{\text{hist}}, Z_i = \{X_i^{(1)}\}$	$X_i^{(2)}$	$\tilde{X}_q^{\text{hist}}, Z_q = \{X_q^{(1)}\}$	$\hat{X}_q^{(2)}$	✓	✗

* Classification does not have $Z_i^{\text{fut}}, Z_q^{\text{fut}}$ covariates; ** $\tilde{X}_i^{\text{hist}}$ is a linear combination of $X_i^{(1)}, X_i^{(2)}$; $\tilde{X}_q^{\text{hist}}$ is a linear combination of $X_q^{(1)}, X_q^{(2)}$

We refer to this training procedure as *amortized meta-learning*: the model is meta-trained across a distribution of tasks, and task adaptation is amortized into a single forward pass conditioned on demonstrations.

4.4. Meta-Training Task Classes

We meta-train the model on a collection of time-series tasks that are directly analogous to the self-supervised and supervised objectives used to train large language models (Table 2). Each task defines a mapping from ICL demonstrations to a *query* prediction and are constructed from raw univariate or multivariate time series with or without covariates.

Below we describe how each task is constructed from raw data and instantiated within the in-context learning prompt.

4.4.1. FORECASTING (ANALOGOUS TO NEXT-TOKEN PREDICTION).

The forecasting task trains the model to predict future values given historical context, mirroring next-token prediction in language models.

Data generation. Given a raw time series $X = \{x_t\}_{t=1}^T$, we sample a window of length L and define:

$$X^{\text{hist}} = X_{t:t+L}, \quad X^{\text{fut}} = X_{t+L:t+L+H},$$

where H is the forecast horizon. If covariates Z are available, we slice them analogously, including future covariates Z^{fut} when known.

ICL instantiation. Each example \mathcal{E}_i provides a historical–future pair $(X_i^{\text{hist}}, Z_i^{\text{hist}}, Z_i^{\text{fut}}) \mapsto X_i^{\text{fut}}$. The query \mathcal{Q} contains only $(X_q^{\text{hist}}, Z_q^{\text{hist}}, Z_q^{\text{fut}})$, and the model predicts $Y_q^{\text{fut}} = X_q^{\text{fut}}$.

4.4.2. IMPUTATION / RECONSTRUCTION (ANALOGOUS TO MASKED SPAN PREDICTION).

This task trains the model to reconstruct missing segments of a time series, analogous to span corruption in encoder–decoder language models.

Data generation. Given a valid window X , we sample a binary mask $M \in \{0, 1\}^T$ using random patch masking, and construct a corrupted input:

$$\tilde{X} = X \odot (1 - M).$$

The mask M is provided as an additional covariate to indicate missingness.

ICL instantiation. Examples demonstrate reconstruction by mapping corrupted inputs to clean outputs. For the query, masked values are withheld and the model predicts $Y_q^{\text{fut}} = X_q^{\text{hist}}$, corresponding to the full reconstructed series.

4.4.3. ANOMALY DETECTION (ANALOGOUS TO DENOISING).

This task trains the model to recover a clean signal from corrupted or anomalous input time-series.

Data generation. Starting from a clean series X , we inject synthetic anomalies such as spikes, level shifts, or additive noise to obtain:

$$X^{\text{corr}} = X + \epsilon,$$

where ϵ denotes structured noise.

ICL instantiation. Examples demonstrate the mapping from corrupted to clean series. For the query, the corrupted segment is withheld, and the model predicts a corrected output $Y_q^{\text{fut}} = X_q^{\text{hist}}$. At inference time, anomaly detection is performed by comparing the model’s prediction or prediction intervals against observed values.

4.4.4. PROPERTY PREDICTION / CLASSIFICATION (ANALOGOUS TO SEQUENCE CLASSIFICATION).

This task trains the model to identify global properties of a time series, such as seasonality, trend, and regime.

Data generation. Labels are obtained from raw data via: (i) synthetic generator KernelSynth (Ansari et al., 2024) that produce series with known properties (kernels), (ii) introducing synthetic properties into series - Censor Augmentation and Spike Injection (Auer et al., 2025), (iii) statistical tests with feature-based heuristics (e.g., seasonality, stability, trend strength) using methods in (Yang et al., 2024), and (iv) clustering of time-series into classes using dataset-domain as seeds (Saha et al., 2022).

Class labels are encoded as constant target series: $X_i^{\text{fut}} = c_i \cdot \mathbf{1}$, where c_i is a class-specific scalar.

ICL instantiation. Since the model predicts time-series outputs, class labels are encoded as constant target series: $Y^{\text{fut}} = c \cdot \mathbf{1}$, where c is a class-specific scalar.

Examples demonstrate different label mappings, and the query prediction corresponds to the inferred class.

4.4.5. SOURCE DE-MIXING (ANALOGOUS TO UNSHUFFLING / SEPARATION).

This task trains the model to separate mixed signals into constituent components, analogous to unshuffling or source separation objectives in NLP and vision.

Data generation. Given two source time-series components $X^{(1)}, X^{(2)}$ we construct a mixed target series $\tilde{X} = w_1 X^{(1)} + w_2 X^{(2)}$, where w_1, w_2 are mixing coefficients. One source component (e.g., $X^{(1)}$) is provided as a covariate, $Z = \{X^{(1)}\}$, while the mixed signal \tilde{X} is treated as the target input.

ICL instantiation. Each example \mathcal{E}_i demonstrates how to recover a component from a mixture:

$$(X_i^{\text{hist}} = \tilde{X}_i^{\text{hist}}, Z_i^{\text{hist}} = \{X_i^{(1), \text{hist}}\}) \mapsto X_i^{\text{fut}} = X_i^{(2), \text{fut}}.$$

The query \mathcal{Q} contains a mixed target series $\tilde{X}_q^{\text{hist}}$ and the known source component $Z_q^{\text{hist}} = \{X_q^{(1), \text{hist}}\}$.

The model predicts $Y_q^{\text{fut}} = X_q^{(2), \text{fut}}$, corresponding to the remaining unmixed component, or equivalently the residual $\tilde{X}_q^{\text{fut}} - w_1 X_q^{(1), \text{fut}}$ when future covariates are available.

4.5. Inference and Task Adaptation

The model, with its fixed parameters θ , infers the time-series task at hand solely through conditioning on in-context demonstrations provided in the prompt \mathcal{P} . Formally, given a set of example demonstrations $\mathcal{S} = \{\mathcal{E}_i\}_{i=1}^N$ and a query

\mathcal{Q} , the model predicts:

$$\hat{Y}_q^{\text{fut}} = f_\theta(\mathcal{P}),$$

where $\mathcal{P} = \text{Ser}(\mathcal{E}_1) \oplus \dots \oplus \text{Ser}(\mathcal{E}_N) \oplus \text{Ser}(\mathcal{Q})$ and the examples implicitly specify the task to be performed.

Forecasting. For forecasting, the query \mathcal{Q} is formed as $\mathcal{Q} = (X_q^{\text{hist}}, Z_q^{\text{hist}}, Z_q^{\text{fut}})$, and the target is $Y_q^{\text{fut}} = X_q^{\text{fut}}$. Each example \mathcal{E}_i demonstrates a forecasting mapping: $\mathcal{E}_i = (X_i^{\text{hist}}, Z_i^{\text{hist}}, X_i^{\text{fut}}, Z_i^{\text{fut}})$.

If external demonstrations are available (e.g., from related time series or domains), they are provided directly as examples. When no external examples are available, one or more examples may be constructed from the query time series itself by sampling historical windows:

$$X_i^{\text{hist}} = X_q[t_i : t_i + L], \quad X_i^{\text{fut}} = X_q[t_i + L : t_i + L + H],$$

with corresponding covariate slices. These windows may partially or fully overlap with the query history, enabling zero-shot forecasting.

Classification. For classification, the query is defined as $\mathcal{Q} = (X_q^{\text{hist}}, Z_q^{\text{hist}})$, and the target output corresponds to a class label encoded as a constant future target series: $Y_q^{\text{fut}} = c \cdot \mathbf{1}$, where c denotes a class-specific scalar.

Each example \mathcal{E}_i demonstrates a labeled mapping: $\mathcal{E}_i = (X_i^{\text{hist}}, Z_i^{\text{hist}}, X_i^{\text{fut}})$, where X_i^{fut} encodes the class label. To ensure unambiguous task specification, the example set \mathcal{S} must contain at least one demonstration for each class.

Anomaly detection. Anomaly detection at inference time is formulated as a forecasting-based comparison task. Given a query time series X_q , we select a segment of interest $[t^* : t^* + H]$ and form:

$$X_q^{\text{hist}} = X_q[: t^*], \quad X_q^{\text{fut}} = X_q[t^* : t^* + H].$$

The query \mathcal{Q} contains $(X_q^{\text{hist}}, Z_q^{\text{hist}}, Z_q^{\text{fut}})$, and the model predicts \hat{Y}_q^{fut} using example demonstrations constructed analogously to the forecasting case. Anomalies are detected by comparing the observed values X_q^{fut} against the predicted distribution \hat{Y}_q^{fut} , using quantile thresholds.

Scope of inference tasks. We evaluate forecasting, classification, and anomaly detection at inference time. Other tasks, such as imputation, reconstruction, and source demixing, primarily serve as self-supervised objectives during training. While these tasks improve representation quality and in-context learning capability, they are not directly evaluated at inference time due to the difficulty of specifying them solely through demonstrations in practical settings.

4.6. Curriculum Learning

Both the proposed architecture and training objective exhibit varying levels of complexity. The hierarchical attention fusion stack progressively aggregates information from individual time-series representations to cross-example rule extraction, while amortized meta-learning exposes the model to a distribution of time-series tasks with increasing functional difficulty. To stabilize optimization and improve generalization, we adopt a curriculum learning strategy (Elman, 1993; Sanger, 2002; Bengio et al., 2009; Wu et al., 2020).

Concretely, we begin training with shorter contexts, fewer in-context examples, and simpler tasks (forecasting and imputation), and gradually increases context length, number of demonstrations, and task complexity to include anomaly detection, classification, and source de-mixing. In parallel, the mixture-of-experts decoder is initialized with uniform expert weights and gradually learns adaptive gating. This curriculum improves convergence speed and final performance by aligning the difficulty of the learning problem with the evolving representational capacity of the model. This has also been shown to benefit in-context learning in Transformers (Garg et al., 2022).

5. Training Data

Recent work has shown that the scale, diversity, and structure of training data are often more critical to foundation-model performance than architectural choices alone. Motivated by this observation, and enabled by the availability of large-scale time-series corpora (Woo et al., 2024; Ansari et al., 2024; Aksu et al., 2024), we construct a diverse training dataset designed to support instruction-conditioned in-context learning across heterogeneous time-series tasks.

5.1. Base corpora.

We incorporate a subset of datasets from the Chronos pre-training corpus (Ansari et al., 2024) and the GIFT-Eval pretraining corpus (Aksu et al., 2024). To maintain compatibility with recent evaluation benchmarks such as fev-bench (Shchur et al., 2025), we carefully exclude datasets that appear in the downstream test sets. The Chronos corpus contributes approximately 30 million univariate time series, spanning diverse domains and temporal granularities. From the GIFT-Eval pretraining corpus, we include approximately 2.5 million additional time series.

5.2. Data augmentation and synthesis.

To increase diversity and induce controllable relationships, we augment the base corpora using three complementary strategies.

Time-series mixup augmentation (TSMixup). First, we apply the TSMixup (Ansari et al., 2024) procedure introduced in Chronos, which generates synthetic mixtures of time series to increase diversity and induce compositional structure. For each augmented sample, we first draw a random integer $k \sim \mathcal{U}\{1, K\}$, and a segment length $\ell \sim \mathcal{U}\{\ell_{\min}, \ell_{\max}\}$. We then sample k univariate time-series segments. To ensure compatibility across different magnitudes and scales, each segment is normalized using z-score scaling. Mixing weights λ are sampled from a symmetric Dirichlet distribution, $\lambda \sim \text{Dir}(\alpha)$, and the augmented series is formed as a convex combination:

$$x_{1:\ell}^{\text{TSMixup}} = \sum_{i=1}^k \lambda_i \tilde{x}_{1:\ell}^{(i)}.$$

In our implementation, we set $K = 3$, $\ell_{\min} = 128$, $\ell_{\max} = 2048$, and $\alpha = 1.5$, and generate approximately 30 million augmented univariate time series. Unlike prior usage focused primarily on forecasting, these mixed series later serve as inputs for multiple task classes, including source de-mixing and anomaly correction.

Kernel-based synthetic generation (KernelSynth). Second, we synthetic time series generated using the KernelSynth (Ansari et al., 2024) procedure from Chronos, to further enrich the training distribution with controlled temporal structures. It is a Gaussian-process-based synthetic data generator which constructs a covariance function by randomly composing kernels from a bank \mathcal{K} , including Linear (trend), RBF (smooth local variation), Periodic (seasonality), Rational Quadratic (multi-scale variation), White Noise, and Constant kernels. For each synthetic instance, we sample a number of basis kernels and compose them using random binary operations $op \in \{+, \times\}$, where addition corresponds to superposition of independent processes and multiplication induces interactions (e.g., modulating seasonality by trend). This yields a composite kernel function $\kappa(t, t')$. A synthetic time series is then sampled from a Gaussian process:

$$x \sim \mathcal{GP}(0, \kappa(t, t'))$$

Using this procedure, we generate approximately 10 million synthetic univariate time series with diverse spectral and structural properties.

Multivariate construction with covariate relations.

Third, leveraging the augmented univariate corpus, we construct multivariate time series with endogenous and exogenous covariate relationships using a custom multivariate generation pipeline. The methodology is described in 5.2.1 This yields approximately 50 million multivariate series with varying numbers of targets and covariates.

5.2.1. MULTIVARIATE CONSTRUCTION WITH COVARIATE RELATIONS.

To generate multivariate time series with structured endogenous and exogenous dependencies, we introduce a multivariate construction pipeline that imposes explicit mathematical relationships between independently sampled univariate series. The goal is to synthesize entangled systems in which target components (*endogenous*) depend on auxiliary drivers (*exogenous*) through a diverse family of causal, nonlinear, and temporally lagged transformations.

Initialization and normalization. We begin by sampling a set of N independent univariate time-series segments

$$\{x^{(1)}, \dots, x^{(N)}\}, \quad x^{(i)} \in \mathbb{R}^L,$$

from a source pool (e.g., real data, TSMixup, or Kernel-Synth). The segment length L is sampled randomly, and each series is sliced using a cyclic iterator to ensure uniform coverage.

To enable stable mathematical composition across heterogeneous magnitudes, each series is normalized by its mean absolute value:

$$\tilde{x}_t^{(i)} = \frac{x_t^{(i)}}{\frac{1}{L} \sum_{s=1}^L |x_s^{(i)}|}.$$

Role assignment. The normalized series are partitioned into:

- endogenous (target) subsets and
- exogenous (covariate) subsets.

We enforce that at least 60% of the components are assigned as endogenous. Exogenous components may influence endogenous ones, but not vice versa, thereby enforcing a causal direction consistent with forecasting settings.

Time-dependent transformations. We introduce time-dependent dependencies by modifying target series over aligned time intervals $[t_{\text{start}}, t_{\text{end}}]$ using a selected base series x_{base} , which may be endogenous or exogenous. For a target series y , we apply one or more of the following transformations:

Linear combination.

$$y_t \leftarrow \alpha x_{\text{base},t} + \beta y_t + \epsilon_t, \quad \epsilon_t \sim \mathcal{N}(0, \sigma^2),$$

where we use $\alpha \sim \mathcal{U}(0.3, 0.6)$, $\beta \sim \mathcal{U}(0.3, 0.7)$, and σ is set to 10% of the standard deviation of the base segment.

Nonlinear modulation.

$$y_t \leftarrow y_t + \gamma f(x_{\text{base},t}),$$

where γ is a scaling coefficient and $f(\cdot)$ is sampled from a library of nonlinear functions, including logarithmic, exponential, power-law, and hyperbolic tangent transformations.

Trend modification. We estimate the linear trend of y as $m_{\text{old}}t + c$ and replace it with a modified trend:

$$y_t^{\text{new}} = (y_t - m_{\text{old}}t - c) + m_{\text{new}}t,$$

where m_{new} is obtained by increasing, decreasing, or reversing the original slope.

Seasonality injection. A sinusoidal component is injected with amplitude modulated by the base series:

$$S_t = A \sin\left(\frac{2\pi t}{P}\right) (1 + \alpha \cdot \text{norm}(x_{\text{base},t})), \quad y_t \leftarrow y_t + S_t.$$

We use $\alpha = 0.3$.

Shock injection. Discrete shocks are added synchronously across target series:

$$y_t \leftarrow y_t + s \cdot M \cdot d(t),$$

where $s \in \{\pm 1\}$, M is the shock magnitude, and $d(t)$ is a decay function (constant, linear, or exponential).

Time-lagged transformations. To induce temporal dependencies, we introduce lagged relationships between a leader series x_{leader} and a follower series y_{follower} .

Lagged influence.

$$y_{\text{follower},t} \leftarrow y_{\text{follower},t} + \alpha x_{\text{leader},t-\ell}.$$

Cointegration (error correction).

$$\epsilon_t = y_{\text{follower},t} - x_{\text{leader},t}, \quad y_{\text{follower},t} \leftarrow y_{\text{follower},t} - \lambda \epsilon_{t-\ell}.$$

Granger-style influence.

$$y_{\text{follower},t} \leftarrow y_{\text{follower},t} + \sum_{k=1}^K \alpha e^{-\beta k} x_{\text{leader},t-k}.$$

Stabilization and output. To prevent numerical instability, all series are clipped to lie within ± 5 standard deviations of their empirical mean. The final output consists of a multivariate target set X , a covariate set Z , and metadata describing the induced dependencies. These constructed systems serve as inputs for downstream instruction-conditioned meta-training tasks.

5.3. Final training mixture.

Across all sources, we obtain a pool of approximately 66 million univariate and multivariate time series. During training, series are sampled from this pool using a fixed mixture:

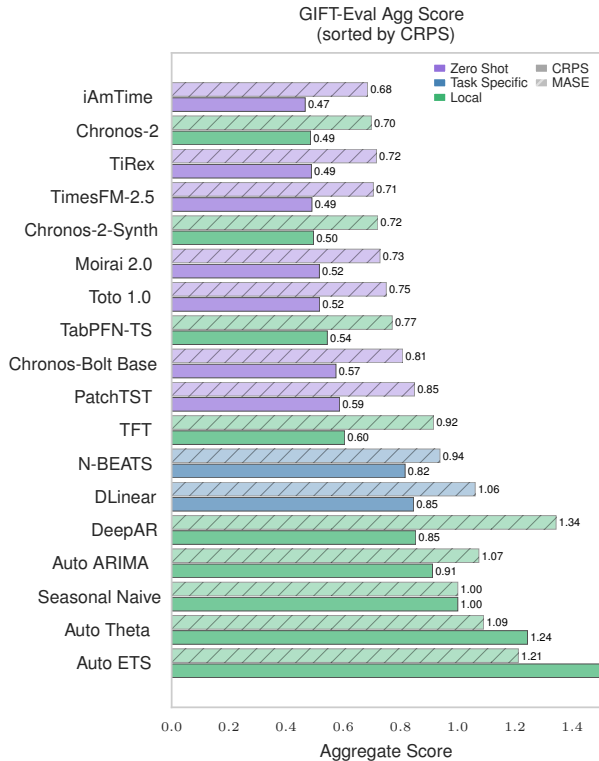


Figure 1. Results of the GIFT-Eval benchmark: Aggregated scores of the overall benchmark. Lower values are better. "Zero-shot Models" are not trained on this data. The In-domain Models are partly trained on the dataset (Overlap:: Moirai 2.0 19%, TimesFM-2.5 10%, TTM: 16%).

10% KernelSynth-generated series, 50% multivariate series with covariates, and 40% univariate series. These series are then used to construct instruction-conditioned in-context prompts for the meta-training task classes described in Section 4.4.

This combination of large-scale real data, structured augmentation, and synthetic generation enables the model to observe a wide distribution of temporal patterns, structural configurations, and task semantics, which is essential for robust amortized meta-learning and in-context task adaptation.

6. Experiments

We evaluate the proposed instruction-conditioned in-context time-series model across a diverse set of large-scale forecasting benchmarks. Our goals are to assess (i) zero-shot forecasting performance across domains, frequencies, and horizons, (ii) probabilistic calibration, and (iii) robustness relative to strong time-series foundation models and classical statistical baselines.

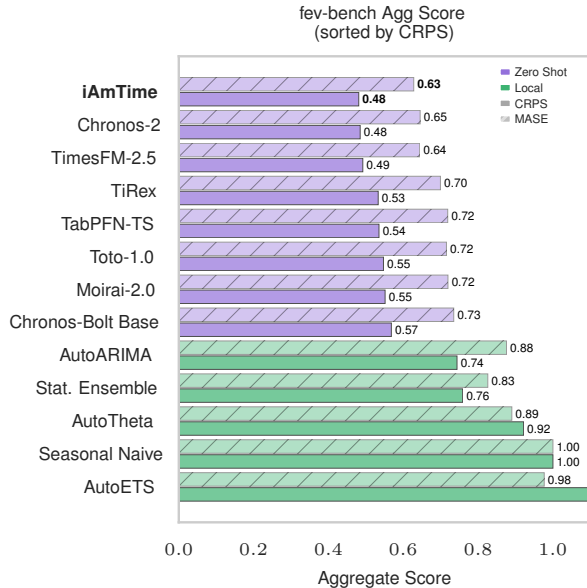


Figure 2. Results of the fev-bench benchmark: Aggregated scores of the overall benchmark. Lower values are better. "Zero-shot Models" are not trained on this data.

6.1. Benchmarks

We conduct experiments on two comprehensive forecasting benchmarks that are widely used to evaluate time-series foundation models.

fev-bench. fev-bench (Shchur et al., 2025) consists of 100 forecasting tasks spanning diverse real-world domains and data characteristics. The benchmark includes tasks with and without covariates and provides the most comprehensive coverage of forecasting scenarios among existing evaluations. None of the datasets or tasks in fev-bench were included in the training corpus of our model.

GIFT-Eval. The GIFT-Eval benchmark (Aksu et al., 2024) comprises 24 datasets evaluated across multiple configurations, including short-, medium-, and long-term forecasting horizons and different temporal granularities. In total, GIFT-Eval defines 97 evaluation settings. We ensure that the pretraining corpus used for our model does not overlap with the test portions of any GIFT-Eval task.

6.2. Baselines

We compare against state-of-the-art time-series foundation models that report strong performance on these benchmarks, including: Chronos-2 (Ansari et al., 2025), TiRex (Auer et al., 2025), TimesFM-2.5 (Das et al., 2024a), Toto-1.0 (Cohen et al., 2025), Moirai-2.0 (Woo et al., 2024), TabPFN-TS (Hoo et al., 2025), and Chronos-Bolt (Ansari et al., 2024).

Table 5. The average win rate and skill score with respect to WQL metric, on the fev-bench dataset. Higher values are better for both. Baseline results and the imputation strategy for handling data leakage in certain tasks are both taken from Shchur et al. 2025.

Model	Avg. Win Rate (%)	Skill Score (%)	Median runtime (s)	Leakage (%)
iAmTime	81.3	51.9	4.8	0
Chronos-2	79.7	51.5	2.7	0
TimesFM-2.5	69.0	50.8	16.9	10
TiRex	66.2	46.7	1.4	1
Toto-1.0	57.3	45.3	90.7	8
TabPFN-TS	52.4	45.8	305.5	0
Moirai-2.0	50.9	44.9	2.5	28
Chronos-Bolt Base	45.2	43.2	1.0	0
Stat. Ensemble	28.3	21.8	690.6	0
AutoARIMA	25.4	23.4	186.8	0
AutoETS	19.1	-27.0	17.0	0
AutoTheta	13.3	7.8	9.3	0
Seasonal Naive	8.3	0.0	2.3	0

As additional baselines, we include classical statistical forecasting methods: AutoARIMA, AutoETS, AutoTheta, and their ensemble (Petropoulos & Svetunkov, 2020), representing well-established approaches from the statistical forecasting literature (Hyndman & Athanasopoulos, 2018).

6.3. Evaluation Metrics

We follow the official evaluation protocols of each benchmark. Point forecast accuracy is measured using mean absolute scaled error (MASE), while probabilistic performance is evaluated using the continuous ranked probability score (CRPS). In practice, CRPS is approximated by the mean weighted quantile loss (WQL) computed over nine quantiles: $Q = \{0.1, 0.2, \dots, 0.9\}$.

To aggregate results across, each evaluation score is normalized by the seasonal naive baseline. Following (Shchur et al., 2025), we additionally report average win rates (W) and skill scores (S). The win rate measures the fraction of pairwise comparisons in which a model outperforms other methods, while the skill score reflects the average percentage improvement over the seasonal naive baseline.

6.4. Results

Across all two benchmarks, the proposed model achieves competitive or superior performance relative to strong foundation-model baselines. We observe consistent improvements in both point and probabilistic forecasting metrics, particularly on tasks involving heterogeneous structures, covariates, and longer horizons. Notably, our model demonstrates strong zero-shot performance without task-specific fine-tuning, indicating effective in-context task adaptation and amortized meta-learning provide advantages beyond scaling historical context alone.

Table 6. Aggregated scores of the overall GIFT-Eval benchmark on the short-, medium-, and long-term performances (top 5 models).

Term length	Model	MASE	CRPS	CRPS Rank
long	iAmTime	0.739	0.451	3.095
	TiRex	0.767	0.467	5.190
	Chronos-2	0.757	0.472	5.571
	TimesFM-2.5	0.751	0.475	5.190
	Chronos-2-Synth	0.792	0.492	7.762
medium	iAmTime	0.716	0.451	4.048
	Chronos-2-Synth	0.747	0.470	7.048
	Chronos-2	0.725	0.471	4.857
	TimesFM-2.5	0.724	0.472	5.571
	TiRex	0.750	0.474	5.286
short	iAmTime	0.654	0.479	3.673
	Chronos-2	0.667	0.496	5.436
	TiRex	0.685	0.502	5.564
	TimesFM-2.5	0.681	0.504	6.673
	Chronos-2-Synth	0.685	0.508	6.891

Fig 2 shows that on fev-bench, iAmTime achieves the strongest overall performance among all evaluated methods. It attains the lowest aggregate CRPS and MASE scores across the 100 forecasting tasks, outperforming recent time-series foundation models. Notably, this performance is achieved in a fully zero-shot setting. Classical statistical methods (AutoARIMA, AutoETS, AutoTheta, and their ensemble) perform substantially worse, highlighting the advantage of large-scale pretraining and contextual adaptation. Also, in Table 5, iAmTime outperforms all models by a substantial margin on this benchmark that includes univariate, multivariate, and covariate-informed forecasting tasks.

On GIFT-eval iAmTime achieves the lowest aggregate CRPS and among the lowest MASE scores (Fig 1), outperforming all other foundation-model baselines. In contrast, task-specific deep learning models (e.g., N-BEATS, DLinear, DeepAR) and classical baselines lag significantly behind, particularly in probabilistic forecasting. Table 6 also shows iAmTime outperforms all competing methods across short- and long-term forecasting tasks.

Results for additional forecasting metrics are provided in the Appendix B.

6.5. Ablation Study

Table 11,12 in Appendix C presents an ablation study on fev-bench evaluating the contributions of instruction-conditioned in-context learning components. Removing in-context examples during training (iAmTime-NoExmp) leads to a substantial drop in win rate and skill score, indicating that learning from demonstration structure is critical. Eliminating semantic tokens (iAmTime-NoToks) causes the largest degradation in skill score, highlighting the importance of explicit role and boundary encoding for stable

task inference. Training without meta-learning objectives (iAmTime-NoMeta), i.e., using forecasting-only supervision, also significantly reduces performance, confirming the benefit of multi-task amortized meta-learning. Together, these results show that examples, semantic tokenization, and instruction-conditioned training are all essential for achieving strong and robust in-context adaptation.

Impact Statement

This work advances time-series modeling by introducing instruction-conditioned in-context learning as a general mechanism for adapting foundation models to new forecasting and analysis tasks without retraining. By enabling flexible task specification through contextual demonstrations, the proposed approach has the potential to reduce the cost and latency associated with deploying and maintaining specialized models across domains such as energy systems, supply-chain planning, healthcare monitoring, and financial risk management. The methodology may also encourage more reusable and data-efficient forecasting systems, particularly in settings where labeled data or retraining infrastructure is limited.

At the same time, as with other large-scale predictive models, the approach inherits limitations related to data quality, representativeness, and downstream decision-making. Forecasts and anomaly signals produced by the model should be used as decision support rather than automated control, especially in high-stakes applications. Future work should explore robustness, interpretability, and responsible deployment practices to mitigate potential misuse and unintended consequences.

References

- Aksu, T., Woo, G., Liu, J., Liu, X., Liu, C., Savarese, S., Xiong, C., and Sahoo, D. Gift-eval: A benchmark for general time series forecasting model evaluation. *arXiv preprint arXiv:2410.10393*, 2024.
- Ansari, A. F., Stella, L., Turkmen, C., Zhang, X., Mercado, P., Shen, H., Shchur, O., Rangapuram, S. S., Arango, S. P., Kapoor, S., et al. Chronos: Learning the language of time series. *arXiv preprint arXiv:2403.07815*, 2024.
- Ansari, A. F., Shchur, O., Küken, J., Auer, A., Han, B., Mercado, P., Rangapuram, S. S., Shen, H., Stella, L., Zhang, X., et al. Chronos-2: From univariate to universal forecasting. *arXiv preprint arXiv:2510.15821*, 2025.
- Audibert, J., Michiardi, P., Guyard, F., Marti, S., and Zuluaga, M. A. Usad: Unsupervised anomaly detection on multivariate time series. In *Proceedings of the 26th ACM SIGKDD international conference on knowledge discovery & data mining*, pp. 3395–3404, 2020.
- Auer, A., Podest, P., Klotz, D., Böck, S., Klambauer, G., and Hochreiter, S. Tirez: Zero-shot forecasting across long and short horizons with enhanced in-context learning. *arXiv preprint arXiv:2505.23719*, 2025.
- Bengio, Y., Louradour, J., Collobert, R., and Weston, J. Curriculum learning. In *Proceedings of the 26th annual international conference on machine learning*, pp. 41–48, 2009.
- Box, G. E. and Jenkins, G. M. Some recent advances in forecasting and control. *Journal of the Royal Statistical Society. Series C (Applied Statistics)*, 17(2):91–109, 1968.
- Brown, T., Mann, B., Ryder, N., Subbiah, M., Kaplan, J. D., Dhariwal, P., Neelakantan, A., Shyam, P., Sastry, G., Askell, A., et al. Language models are few-shot learners. *Advances in neural information processing systems*, 33: 1877–1901, 2020.
- Cao, W., Wang, D., Li, J., Zhou, H., Li, L., and Li, Y. Brits: Bidirectional recurrent imputation for time series. *Advances in neural information processing systems*, 31, 2018.
- Challu, C., Olivares, K. G., Oreshkin, B. N., Ramirez, F. G., Canseco, M. M., and Dubrawski, A. Nhits: Neural hierarchical interpolation for time series forecasting. In *Proceedings of the AAAI conference on artificial intelligence*, volume 37, pp. 6989–6997, 2023.
- Cohen, B., Khwaja, E., Doubli, Y., Lemaachi, S., Lettieri, C., Masson, C., Miccinilli, H., Ramé, E., Ren, Q., Ros-tamizadeh, A., et al. This time is different: An observability perspective on time series foundation models. *arXiv preprint arXiv:2505.14766*, 2025.
- Das, A., Faw, M., Sen, R., and Zhou, Y. In-context fine-tuning for time-series foundation models. *arXiv preprint arXiv:2410.24087*, 2024a.
- Das, A., Kong, W., Sen, R., and Zhou, Y. A decoder-only foundation model for time-series forecasting. In *Forty-first International Conference on Machine Learning*, 2024b.
- Dosovitskiy, A. An image is worth 16x16 words: Transformers for image recognition at scale. *arXiv preprint arXiv:2010.11929*, 2020.
- Elman, J. L. Learning and development in neural networks: The importance of starting small. *Cognition*, 48(1):71–99, 1993.
- Evgeniou, T. and Pontil, M. Regularized multi-task learning. In *Proceedings of the tenth ACM SIGKDD international conference on Knowledge discovery and data mining*, pp. 109–117, 2004.

- Fawaz, H. I. Deep learning for time series classification. *arXiv preprint arXiv:2010.00567*, 2020.
- Finn, C., Abbeel, P., and Levine, S. Model-agnostic meta-learning for fast adaptation of deep networks. In *International conference on machine learning*, pp. 1126–1135. PMLR, 2017.
- Garg, S., Tsipras, D., Liang, P. S., and Valiant, G. What can transformers learn in-context? a case study of simple function classes. *Advances in neural information processing systems*, 35:30583–30598, 2022.
- Gneiting, T. and Katzfuss, M. Probabilistic forecasting. *Annual Review of Statistics and Its Application*, 1(1):125–151, 2014.
- Haviv, A., Ram, O., Press, O., Izsak, P., and Levy, O. Transformer language models without positional encodings still learn positional information. *arXiv preprint arXiv:2203.16634*, 2022.
- Holtzman, A., West, P., Shwartz, V., Choi, Y., and Zettlemoyer, L. Surface form competition: Why the highest probability answer isn’t always right. *arXiv preprint arXiv:2104.08315*, 2021.
- Hoo, S. B., Müller, S., Salinas, D., and Hutter, F. From tables to time: How tabPFN-v2 outperforms specialized time series forecasting models. *arXiv preprint arXiv:2501.02945*, 2025.
- Hyndman, R. J. and Athanasopoulos, G. *Forecasting: principles and practice*. OTexts, 2018.
- Kim, T., Kim, J., Tae, Y., Park, C., Choi, J.-H., and Choo, J. Reversible instance normalization for accurate time-series forecasting against distribution shift. In *International conference on learning representations*, 2021.
- Lim, B., Arık, S. Ö., Loeff, N., and Pfister, T. Temporal fusion transformers for interpretable multi-horizon time series forecasting. *International journal of forecasting*, 37(4):1748–1764, 2021.
- Lu, J., Sun, Y., and Yang, S. In-context time series predictor. *arXiv preprint arXiv:2405.14982*, 2024.
- Min, S., Lewis, M., Zettlemoyer, L., and Hajishirzi, H. Metaicl: Learning to learn in context. In *Proceedings of the 2022 conference of the North American chapter of the Association for Computational Linguistics: Human Language Technologies*, pp. 2791–2809, 2022.
- Mishra, S., Khashabi, D., Baral, C., and Hajishirzi, H. Cross-task generalization via natural language crowdsourcing instructions. In *Proceedings of the 60th Annual Meeting of the Association for Computational Linguistics (Volume 1: Long Papers)*, pp. 3470–3487, 2022.
- Nie, Y. A time series is worth 64 words: Long-term forecasting with transformers. *arXiv preprint arXiv:2211.14730*, 2022.
- Oreshkin, B. N., Carpio, D., Chapados, N., and Bengio, Y. N-beats: Neural basis expansion analysis for interpretable time series forecasting. *arXiv preprint arXiv:1905.10437*, 2019.
- Petropoulos, F. and Svetunkov, I. A simple combination of univariate models. *International journal of forecasting*, 36(1):110–115, 2020.
- Raffel, C., Shazeer, N., Roberts, A., Lee, K., Narang, S., Matena, M., Zhou, Y., Li, W., and Liu, P. J. Exploring the limits of transfer learning with a unified text-to-text transformer. *Journal of machine learning research*, 21(140):1–67, 2020.
- Rangapuram, S. S., Seeger, M. W., Gasthaus, J., Stella, L., Wang, Y., and Januschowski, T. Deep state space models for time series forecasting. *Advances in neural information processing systems*, 31, 2018.
- Ruder, S. An overview of multi-task learning in deep neural networks. *arXiv preprint arXiv:1706.05098*, 2017.
- Saha, A., Ananthram, A., Allaway, E., Ji, H., and McKeown, K. Seeded hierarchical clustering for expert-crafted taxonomies. In *Findings of the Association for Computational Linguistics: EMNLP 2022*, pp. 1595–1609, 2022.
- Salinas, D., Flunkert, V., Gasthaus, J., and Januschowski, T. Deepar: Probabilistic forecasting with autoregressive recurrent networks. *International journal of forecasting*, 36(3):1181–1191, 2020.
- Sanger, T. D. Neural network learning control of robot manipulators using gradually increasing task difficulty. *IEEE transactions on Robotics and Automation*, 10(3): 323–333, 2002.
- Shchur, O., Ansari, A. F., Turkmen, C., Stella, L., Erickson, N., Gueron, P., Bohlke-Schneider, M., and Wang, Y. fevbench: A realistic benchmark for time series forecasting. *arXiv preprint arXiv:2509.26468*, 2025.
- Vilalta, R. and Drissi, Y. A perspective view and survey of meta-learning. *Artificial intelligence review*, 18(2):77–95, 2002.
- Wei, J., Bosma, M., Zhao, V. Y., Guu, K., Yu, A. W., Lester, B., Du, N., Dai, A. M., and Le, Q. V. Finetuned language models are zero-shot learners. *arXiv preprint arXiv:2109.01652*, 2021.
- Wei, J., Wang, X., Schuurmans, D., Bosma, M., Xia, F., Chi, E., Le, Q. V., Zhou, D., et al. Chain-of-thought prompting

elicits reasoning in large language models. *Advances in neural information processing systems*, 35:24824–24837, 2022.

Woo, G., Liu, C., Kumar, A., Xiong, C., Savarese, S., and Sahoo, D. Unified training of universal time series forecasting transformers. 2024.

Wu, X., Dyer, E., and Neyshabur, B. When do curricula work? *arXiv preprint arXiv:2012.03107*, 2020.

Yang, Z., Ghosh, M., Saha, A., Xu, D., Shmakov, K., and Lee, K.-c. A comprehensive forecasting framework based on multi-stage hierarchical forecasting reconciliation and adjustment. In *2024 IEEE International Conference on Big Data (BigData)*, pp. 1151–1160. IEEE, 2024.

Zeng, A., Chen, M., Zhang, L., and Xu, Q. Are transformers effective for time series forecasting? In *Proceedings of the AAAI conference on artificial intelligence*, volume 37, pp. 11121–11128, 2023.

Zhao, Z., Wallace, E., Feng, S., Klein, D., and Singh, S. Calibrate before use: Improving few-shot performance of language models. In *International conference on machine learning*, pp. 12697–12706. PMLR, 2021.

Zhong, R., Lee, K., Zhang, Z., and Klein, D. Adapting language models for zero-shot learning by meta-tuning on dataset and prompt collections. *arXiv preprint arXiv:2104.04670*, 2021.

A. Datasets

A.1. Training Data

Table 7. List of training datasets used from Chronos pre-training corpus, published by (Ansari et al., 2024)

Name	Domain	# Series	Avg. Length
Mexico City Bikes	Mobility / Transport	494	78,313
Brazilian Cities Temperature	Weather / Climate	12	757
Solar (5 Min.)	Energy	5,166	105,120
Solar (Hourly)	Energy	5,166	105,120
Spanish Energy and Weather	Energy / Weather	66	35,064
Taxi (Hourly)	Mobility / Transport	2,428	739
USHCN	Weather / Climate	6,090	38,653
Weatherbench (Hourly)	Weather / Climate	225,280	350,639
Weatherbench (Daily)	Weather / Climate	225,280	14,609
Weatherbench (Weekly)	Weather / Climate	225,280	2,087
Wiki Daily (100k)	Web / Information	100,000	2,741
Wind Farms (Hourly)	Energy	100,000	8,514
Wind Farms (Daily)	Energy	100,000	354
Electricity (15 Min.)	Energy	370	113,341
Electricity (Hourly)	Energy	321	26,304
Electricity (Weekly)	Energy	321	156
KDD Cup 2018	Energy	270	10,897
London Smart Meters	Energy	5,560	29,951
M4 (Daily)	Business / Economics	4,227	2,371
M4 (Hourly)	Business / Economics	414	901
M4 (Monthly)	Business / Economics	48,000	234
M4 (Weekly)	Business / Economics	359	1,035
Pedestrian Counts	Mobility / Urban	66	47,459
Rideshare	Mobility / Transport	2,340	541
Taxi (30 Min.)	Mobility / Transport	2,428	1,478
Temperature–Rain	Weather / Climate	32,072	725
Uber TLC (Hourly)	Mobility / Transport	262	4,344
Uber TLC (Daily)	Mobility / Transport	262	181

Table 8. Subset of pre-training datasets used from GiftEvalPretrain, published by (Aksu et al., 2024)

Name	Domain	# Series	Avg. Length
azure vm traces 2017	Cloud / Systems	159,472	5,553
borg cluster data 2011	Cloud / Systems	143,386	3,749
bdg-2 panther	Energy	105	8,760
bdg-2 fox	Energy	135	17,219
bdg-2 rat	Energy	280	16,887
bdg-2 bear	Energy	91	16,289
lcl	Energy	713	13,385
smart	Energy	5	19,142
ideal	Energy	217	5,785
sceaux	Energy	1	34,223
borealis	Energy	15	5,551
buildings 900k	Energy	1,795,256	8,761
largest 2017	Climate	8,196	105,120
largest 2018	Climate	8,428	105,120
largest 2019	Climate	8,600	105,120
largest 2020	Climate	8,561	105,408
largest 2021	Climate	8,548	105,120
PEMS03	Transport	358	26,208
PEMS04	Transport	307	16,992
PEMS07	Transport	883	28,224
PEMS08	Transport	170	17,856
PEMS BAY	Transport	325	52,128
LOS LOOP	Transport	207	34,272
BEIJING SUBWAY 30MIN	Transport	276	1,572
SHMETRO	Transport	288	8,809
HZMETRO	Transport	80	2,377
Q-TRAFFIC	Transport	45,148	5,856
subseasonal	Climate	862	16,470
subseasonal precip	Climate	862	11,323
wind power	Energy	1	7,397,147
solar power	Energy	1	7,397,222
kaggle web traffic weekly	Web	14,563	114
kdd2022	Energy	134	35,280
godaddy	Web	3,135	41
favorita sales	Retail	111,840	1,244
china air quality	Environment	437	13,133
beijing air quality	Environment	12	35,064
residential load power	Energy	271	538,725
residential pv power	Energy	233	537,935
cdc fluview ilinet	Healthcare	75	852
cdc fluview who	Healthcare	74	564

A.2. Evaluation Data

A Foundation Model for Instruction-Conditioned In-Context Time Series Tasks

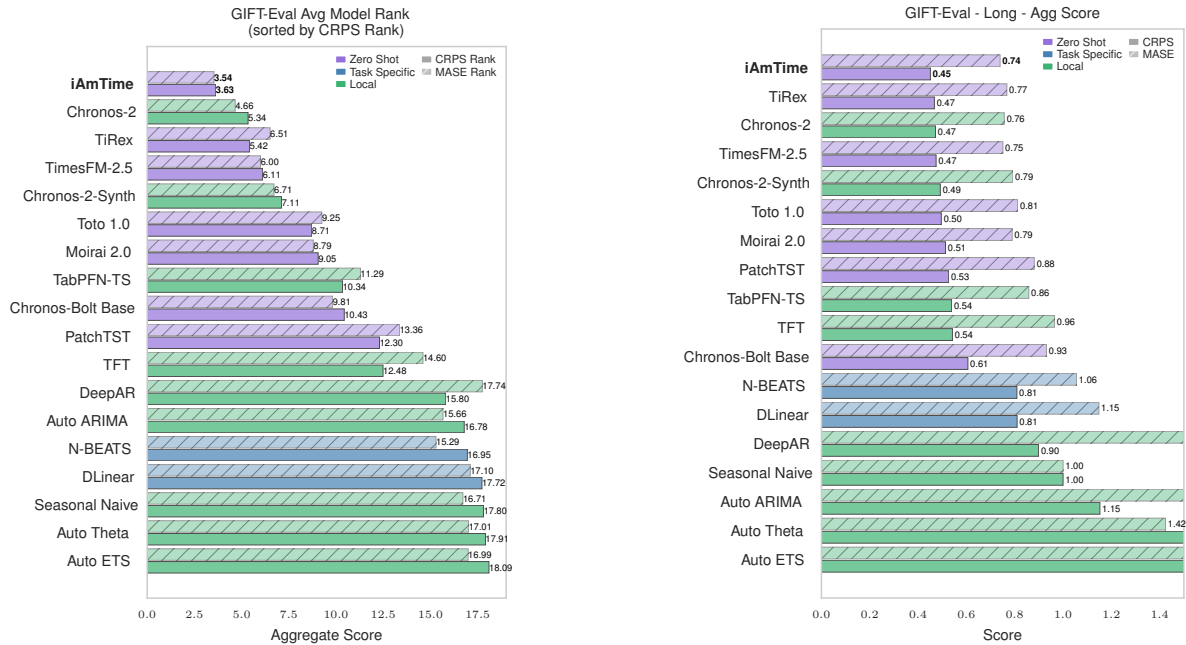
Table 9. Benchmark datasets dataset summary of GIFT-Eval (Aksu et al., 2024). The benchmark provides various settings for evaluating horizons (H) in terms of short/mid/long term forecasts. Each dataset is evaluated over W windows.

Dataset	Domain	Freq.	# Series	Series Length			# Target	Short-term		Med-term		Long-term	
				Avg	Min	Max		Variate	H	W	H	Windows	H
Jena Weather	Nature	10T	1	52,704	52,704	52,704	21	48	20	480	1	720	8
Jena Weather	Nature	H	1	8,784	8,784	8,784	21	48	19	480	2	720	2
Jena Weather	Nature	D	1	366	366	366	21	30	2				
BizTObS - Application	Web/CloudOps	10S	1	8,834	8,834	8,834	2	60	15	600	2	900	1
BizTObS - Service	Web/CloudOps	10S	21	8,835	8,835	8,835	2	60	15	600	2	900	1
BizTObS - L2C	Web/CloudOps	5T	1	31,968	31,968	31,968	7	48	20	480	7	720	5
BizTObS - L2C	Web/CloudOps	H	1	2,664	2,664	2,664	7	48	6	480	1	720	1
Bitbrains - Fast Storage	Web/CloudOps	5T	1,250	8,640	8,640	8,640	2	48	18	480	2	720	2
Bitbrains - Fast Storage	Web/CloudOps	H	1,250	721	721	721	2	48	2				
Bitbrains - rnd	Web/CloudOps	5T	500	8,640	8,640	8,640	2	48	18	480	2	720	2
Bitbrains - rnd	Web/CloudOps	H	500	720	720	720	2	48	2				
Restaurant	Sales	D	807	358	67	478	1	30	1				
ETT1	Energy	15T	1	69,680	69,680	69,680	7	48	20	480	15	720	10
ETT1	Energy	H	1	17,420	17,420	17,420	7	48	20	480	4	720	3
ETT1	Energy	D	1	725	725	725	7	30	3				
ETT1	Energy	W-THU	1	103	103	103	7	8	2				
ETT2	Energy	15T	1	69,680	69,680	69,680	7	48	20	480	15	720	10
ETT2	Energy	H	1	17,420	17,420	17,420	7	48	20	480	4	720	3
ETT2	Energy	D	1	725	725	725	7	30	3				
ETT2	Energy	W-THU	1	103	103	103	7	8	2				
Loop Seattle	Transport	5T	323	105,120	105,120	105,120	1	48	20	480	20	720	15
Loop Seattle	Transport	H	323	8,760	8,760	8,760	1	48	19	480	2	720	2
Loop Seattle	Transport	D	323	365	365	365	1	30	2				
SZ-Taxi	Transport	15T	156	2,976	2,976	2,976	1	48	7	480	1	720	1
SZ-Taxi	Transport	H	156	744	744	744	1	48	2				
M.DENSE	Transport	H	30	17,520	17,520	17,520	1	48	20	480	4	720	3
M.DENSE	Transport	D	30	730	730	730	1	30	3				
Solar	Energy	10T	137	52,560	52,560	52,560	1	48	20	480	11	720	8
Solar	Energy	H	137	8,760	8,760	8,760	1	48	19	480	2	720	2
Solar	Energy	D	137	365	365	365	1	30	2				
Solar	Energy	W-FRI	137	52	52	52	1	8	1				
Hierarchical Sales	Sales	D	118	1,825	1,825	1,825	1	30	7				
Hierarchical Sales	Sales	W-WED	118	260	260	260	1	8	4				
M4 Yearly	Econ/Fin	A-DEC	22,974	37	19	284	1	6	1				
M4 Quarterly	Econ/Fin	Q-DEC	24,000	100	24	874	1	8	1				
M4 Monthly	Econ/Fin	M	48,000	234	60	2,812	1	18	1				
M4 Weekly	Econ/Fin	W-SUN	359	1,035	93	2,610	1	13	1				
M4 Daily	Econ/Fin	D	4,227	2,371	107	9,933	1	14	1				
M4 Hourly	Econ/Fin	H	414	902	748	1,008	1	48	2				
Hospital	Healthcare	M	767	84	84	84	1	12	1				
COVID Deaths	Healthcare	D	266	212	212	212	1	30	1				
US Births	Healthcare	D	1	7,305	7,305	7,305	1	30	20				
US Births	Healthcare	D	1	7,305	7,305	7,305	1	30	20				
US Births	Healthcare	W-TUE	1	1,043	1,043	1,043	1	8	14				
US Births	Healthcare	M	1	240	240	240	1	12	2				
Saugeen	Nature	D	1	23,741	23,741	23,741	1	30	20				
Saugeen	Nature	W-THU	1	3,391	3,391	3,391	1	8	20				
Saugeen	Nature	M	1	780	780	780	1	12	7				
Temperature Rain	Nature	D	32,072	725	725	725	1	30	3				
KDD Cup 2018	Nature	H	270	10,898	9,504	10,920	1	48	20	480	2	720	2
KDD Cup 2018	Nature	D	270	455	396	455	1	30	2				
Car Parts	Sales	M	2,674	51	51	51	1	12	1				
Electricity	Energy	15T	370	140,256	140,256	140,256	1	48	20	480	20	720	20
Electricity	Energy	H	370	35,064	35,064	35,064	1	48	20	480	8	720	5
Electricity	Energy	D	370	1,461	1,461	1,461	1	30	5				
Electricity	Energy	W-FRI	370	208	208	208	1	8	3				

A Foundation Model for Instruction-Conditioned In-Context Time Series Tasks

Table 10. Benchmark datasets dataset summary of fev-bench (Shchur et al., 2025). This benchmark contains 100 tasks including the ones listed here and overlapping tasks from GIFT-Eval on the BizITObs - L2C, ETT, Hierarchical Sales, Hospital, Jena Weather, Loop Seattle, M-DENSE, SZ Taxi, Solar tasks.

Task	Domain	Freq.	H	W	Median length	# series	# targets	# past cov.	# known cov.	# static cov.
Australian Tourism	econ	Q	8	2	36	89	1	0	0	0
FRED-MD - CEE	econ	M	12	20	798	1	3	4	0	0
FRED-MD - Macro	econ	M	12	20	798	1	51	0	0	0
FRED-QD - CEE	econ	Q	8	20	266	1	3	4	0	0
FRED-QD - Macro	econ	Q	8	20	266	1	51	0	0	0
GVAR	econ	Q	8	10	178	33	6	3	0	0
US Consumption	econ	M	12	10	792	31	1	0	0	0
US Consumption	econ	Q	8	10	262	31	1	0	0	0
US Consumption	econ	Y	5	10	64	31	1	0	0	0
World CO2 Emissions	econ	Y	5	9	60	191	1	0	0	0
World Life Expectancy	econ	Y	5	10	74	237	1	0	0	0
World Tourism	econ	Y	5	2	21	178	1	0	0	0
ENTSO-e Load	energy	15T	96	20	175292	6	1	0	3	0
ENTSO-e Load	energy	30T	96	20	87645	6	1	0	3	0
ENTSO-e Load	energy	H	168	20	43822	6	1	0	3	0
EPF-BE	energy	H	24	20	52416	1	1	0	2	0
EPF-DE	energy	H	24	20	52416	1	1	0	2	0
EPF-FR	energy	H	24	20	52416	1	1	0	2	0
EPF-NP	energy	H	24	20	52416	1	1	0	2	0
EPF-PJM	energy	H	24	20	52416	1	1	0	2	0
ERCOT	energy	D	28	20	6452	8	1	0	0	0
ERCOT	energy	H	168	20	154872	8	1	0	0	0
ERCOT	energy	M	12	15	211	8	1	0	0	0
ERCOT	energy	W	13	20	921	8	1	0	0	0
GFC12	energy	H	168	10	39414	11	1	0	1	0
GFC14	energy	H	168	20	17520	1	1	0	1	0
GFC17	energy	H	168	20	17544	8	1	0	1	0
Solar with Weather	energy	15T	96	20	198600	1	1	2	7	0
Solar with Weather	energy	H	24	20	49648	1	1	2	7	0
BOOMLET-1062	cloud	5T	288	20	16384	1	21	0	0	0
BOOMLET-1209	cloud	5T	288	20	16384	1	53	0	0	0
BOOMLET-1225	cloud	T	60	20	16384	1	49	0	0	0
BOOMLET-1230	cloud	5T	288	20	16384	1	23	0	0	0
BOOMLET-1282	cloud	T	60	20	16384	1	35	0	0	0
BOOMLET-1487	cloud	5T	288	20	16384	1	54	0	0	0
BOOMLET-1631	cloud	30T	96	20	10463	1	40	0	0	0
BOOMLET-1676	cloud	30T	96	20	10463	1	100	0	0	0
BOOMLET-1855	cloud	H	24	20	5231	1	52	0	0	0
BOOMLET-1975	cloud	H	24	20	5231	1	75	0	0	0
BOOMLET-2187	cloud	H	24	20	5231	1	100	0	0	0
Favorita Store Sales	retail	M	12	2	54	1579	1	1	1	6
Favorita Store Sales	retail	W	13	10	240	1579	1	1	1	6
Favorita Store Sales	retail	D	28	10	1688	1579	1	1	2	6
Favorita Transactions	retail	M	12	2	54	51	1	1	0	5
Favorita Transactions	retail	W	13	10	240	51	1	1	0	5
Favorita Transactions	retail	D	28	10	1688	51	1	1	1	5
KDD Cup 2022	energy	D	14	10	243	134	1	9	0	0
KDD Cup 2022	energy	10T	288	10	35279	134	1	9	0	0
KDD Cup 2022	energy	30T	96	10	11758	134	1	9	0	0
M5	retail	M	12	1	58	30490	1	0	8	5
M5	retail	W	13	1	257	30490	1	0	8	5
M5	retail	D	28	1	1810	30490	1	0	8	5
Restaurant	retail	D	28	8	296	817	1	0	0	4
Rossmann	retail	W	13	8	133	1115	1	1	4	10
Rossmann	retail	D	48	10	942	1115	1	1	5	10
Walmart	retail	W	39	1	143	2936	1	0	10	4
ECDC ILI	healthcare	W	13	10	201	25	1	0	0	0
Hospital Admissions	healthcare	D	28	20	1731	8	1	0	0	0
Hospital Admissions	healthcare	W	13	16	246	8	1	0	0	0
UK COVID - Nation - Cumulative	healthcare	D	28	20	729	4	3	5	0	0
UK COVID - Nation - New	healthcare	D	28	20	729	4	3	5	0	0
UK COVID - UTLA - Cumulative	healthcare	W	13	5	104	214	1	0	0	0
UK COVID - UTLA - New	healthcare	D	28	10	721	214	1	0	0	0



(a) Overall CRPS and MASE scores on GIFT-Eval. Lower values are better. “Zero-shot Models” are not trained on this data. In-domain models are partly trained.

(b) Aggregated CRPS-Rank and MASE-Rank on long-term GIFT-Eval results. Lower values are better. “Zero-shot Models” are not trained on this data.

Figure 3. Overall and long-term performance on the GIFT-Eval benchmark. (Train-evaluation overlap: Moirai 2.0 19%, TimesFM-2.5 10%, TTM 16%)

B. Extended Evaluations

This section presents additional experimental results complementing Section 6.4.

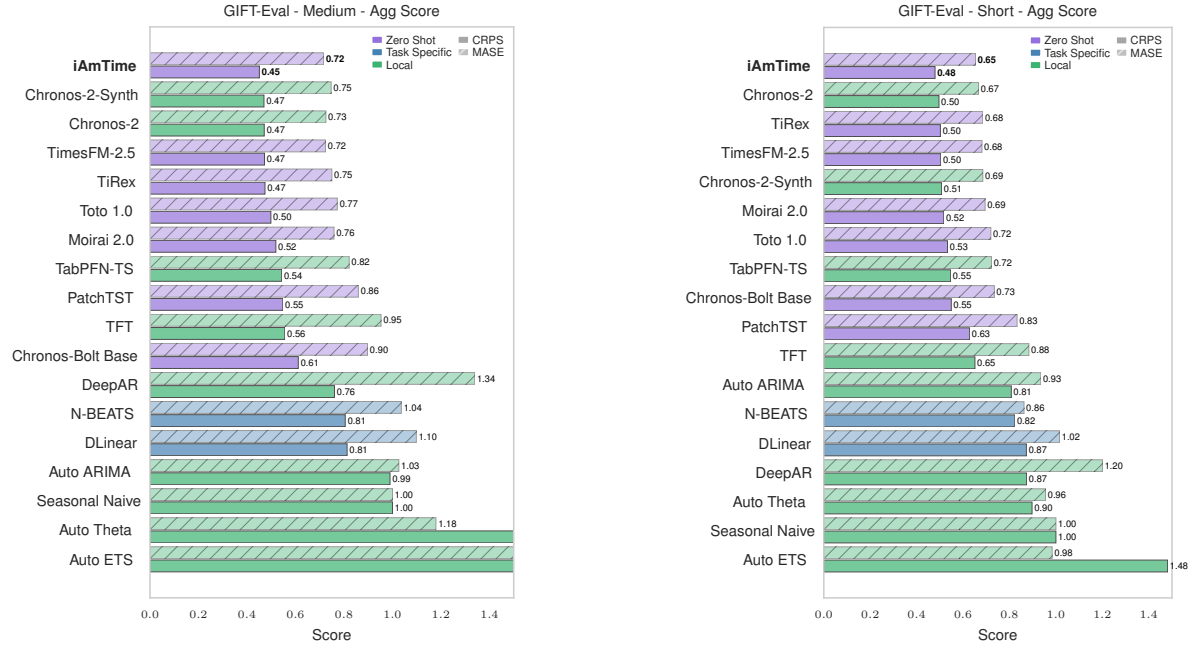
B.1. Zero-shot generalization on GIFT-Eval

First, we talk about the overall CRPS-Rank and MASE-Rank on the zero-shot evaluation of GIFT-Eval benchmark. This rank based metric is helpful as it averages rank across evaluation settings ensure robustness metrics against outlier performance. Followed by this, we show the short-, medium-, long-term, and univariate-multivariate forecasts from GIFT-Eval.

iAmTime achieves the strongest overall performance in the zero-shot setting on GIFT-Eval, attaining the best or near-best aggregated CRPS and MASE ranks across all evaluation slices (Figure 3a). Despite no training on the benchmark data, iAmTime consistently outperforms or matches task-specific and locally trained models, including methods with partial train-evaluation overlap. This advantage persists across long-, medium-, and short-term horizons (Figures 3b,4a,4b) as well as univariate and multivariate inputs (Figures 5a,5b), demonstrating robust zero-shot generalization across diverse forecasting conditions.

Performance trends are stable across evaluation slices and including horizon length. It is also stable across input structure, and to make this point more explicit, Table 14 isolate the performance on only the multivariate subset. In majority of the cases iAmTime achieves the top rank. This indicates robustness to both forecasting horizon and input dimensionality. In contrast, classical statistical baselines and fully local models generally underperform, especially on longer horizons, while other foundation models show competitive but less consistent rankings across settings.

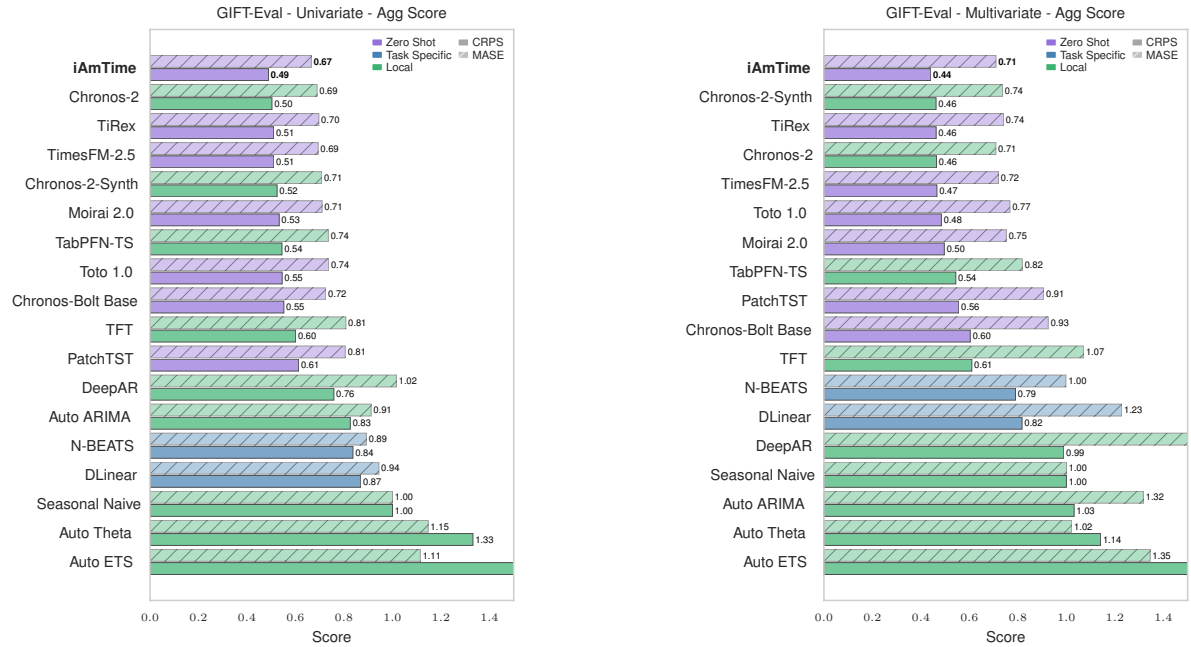
A Foundation Model for Instruction-Conditioned In-Context Time Series Tasks



(a) Aggregated CRPS and MASE scores on medium-term GIFT-Eval results. Lower values are better. “Zero-shot Models” are not trained on this data.

(b) Aggregated CRPS and MASE scores on short-term GIFT-Eval results. Lower values are better. “Zero-shot Models” are not trained on this data.

Figure 4. Term length performance on the GIFT-Eval benchmark. (Train-evaluation overlap: Moirai 2.0 19%, TimesFM-2.5 10%, TTM 16%)



(a) Aggregated CRPS and MASE scores on univariate GIFT-Eval results. Lower values are better. “Zero-shot Models” are not trained on this data.

(b) Aggregated CRPS and MASE scores on multivariate GIFT-Eval results. Lower values are better. “Zero-shot Models” are not trained on this data.

Figure 5. Result on univariate and multivariate inputs on the GIFT-Eval benchmark. (Train-evaluation overlap: Moirai 2.0 19%, TimesFM-2.5 10%, TTM 16%)

C. Ablations

Table 11. Win rate and skill score with respect to MASE on fev-bench dataset. **iAmTime** is the base version trained using Meta-training tasks. **iAmTime-NoExmp** ablates the examples (0 examples) while training (and removes the classification task). **iAmTime-NoToks** ablates the use of semantic tokens while training. **iAmTime-NoMeta** uses only forecasting tasks to train the model.

Model	Win Rate (%)	Skill Score (%)	Median Runtime (s)	Leakage %
iAmTime	86.1	37.2	4.8	0
Chronos-2	79.1	35.5	2.7	0
iAmTime-NoExmp	70.9	32.9	3.4	0
TimesFM-2.5	67.9	35.6	16.9	10
TiRex	62.9	30.1	1.4	1
iAmTime-NoToks	61.3	20.5	4.5	10
iAmTime-NoMeta	59.1	30.6	4.8	8
Toto-1.0	54.8	28.5	90.7	8
Moirai-2.0	46.8	28.1	2.5	28
TabPFN-TS	46.3	27.6	305.5	0
Chronos-Bolt	44.3	26.5	1.0	0
Seasonal Naive	11.2	0.0	2.3	0

Table 12. Metrics sorted with respect to CRPS on the GIFT-Eval dataset. **iAmTime** is the base version trained using Meta-training tasks. **iAmTime-NoExmp** ablates the examples (0 examples) while training (and removes the classification task). **iAmTime-NoToks** ablates the use of semantic tokens while training. **iAmTime-NoMeta** uses only forecasting tasks to train the model.

Model	MASE	MASE Rank	CRPS	CRPS Rank
iAmTime	0.685	3.536	0.467	3.629
Chronos-2	0.698	4.660	0.485	5.340
iAmTime-NoExmp	0.705	6.134	0.487	5.773
TiRex	0.716	6.505	0.488	5.423
TimesFM-2.5	0.705	6.000	0.490	6.113
Chronos-2-Synth	0.720	6.711	0.496	7.113
iAmTime-NoMeta	0.725	8.031	0.500	7.454
Moirai2	0.728	8.794	0.516	9.052
iAmTime-NoToks	0.727	8.014	0.510	7.773
Toto 1.0	0.750	9.247	0.517	8.711
TabPFN-TS	0.771	11.289	0.544	10.340
Chronos-bolt base	0.808	9.814	0.574	10.433
Seasonal Naive	1.000	16.711	1.000	17.804

C.1. Training Method Ablations

To isolate the contributions of instruction-conditioned in-context learning, we evaluate four variants of our model under a controlled training and inference setup to create targeted ablations that remove one component at a time while keeping all other factors fixed. All variants are evaluated under the same inference protocol on fev-bench and GIFT-Eval, allowing us to attribute performance differences directly to the presence or absence of each instruction-conditioned component.

The ablation results in Table 11,12 can be explained by how each component contributes to learning a conditional predictor under the in-context learning formulation.

iAmTime The full model (iAmTime) is trained using heterogeneous meta-training tasks with explicit example–query prompts and structured semantic tokens. This method performs the best on all tasks.

iAmTime-NoExmp Removes example demonstrations during training (i.e., zero in-context examples). Removing example demonstrations during training (iAmTime-NoExmp) deprives the model of explicit input–output pair structure, forcing it to rely solely on implicit temporal patterns rather than learning to infer task mappings from context. As a result, the model cannot internalize the alignment between historical inputs and future outputs that is required for effective in-context adaptation at inference time.

iAmTime-NoMeta Restricts training to forecasting-only supervision, eliminating meta-training across task classes. Training without meta-learning objectives (iAmTime-NoMeta) reduces performance by collapsing the training distribution to a single forecasting task. This prevents the model from learning a distribution over task mappings and forces specialization to a fixed objective, eliminating the amortized adaptation behavior required for general in-context learning.

Together, these findings confirm that instruction-conditioned meta-training, and example-based supervision are not additive heuristics, but jointly necessary to enable reliable in-context task adaptation in time-series models.

C.2. Structural Ablations

iAmTime-NoToks Removes semantic role tokens and relies on raw numeric concatenation. Ablating semantic tokens (iAmTime-NoToks) leads to the largest degradation in skill score because the model loses discrete boundary and role information that separates targets, covariates, examples, and queries. Without these anchors, attention mechanisms are forced to infer structure implicitly from raw numeric sequences, increasing representation leakage and ambiguity in cross-example interactions, which directly undermines the stability of learned task inference.

These ablation setups closely parallels the MetaICL framework (Min et al., 2022), where models are explicitly trained on demonstration–query episodes rather than relying on emergent in-context behavior from scale alone. In MetaICL, removing meta-training or demonstration structure substantially degrades ICL performance, even when model capacity is held fixed. Similarly, our ablations show that eliminating examples, semantic role tokens, or multi-task meta-training collapses the model’s ability to infer task mappings from context. In both cases, effective in-context learning arises not merely from architectural capacity, but from training on structured in-context objectives that align training and inference formats, enabling task adaptation to be amortized into a single forward pass.

C.3. Robustness to Distribution Shift during Inference

To study this, we train the model by selecting subset of data belonging to domain C_T , and perform inference on a non-overlapping subset of domains C_I such that $C_T \cap C_I = \emptyset$. While doing inference, we provide ICL examples from classes C_E in three ways:

- $C_E \subset C_I$,
- $C_E \subset C_T$, and
- repeat 1 but perform perturbations on the example time-series.

Table 13. Results on subset of fev-bench observing the robustness to distribution shift

Inference ICL Variant	Win Rate (%)	Skill Score (%)
$C_E \subset C_I$	71.3	50.1
$C_E \subset C_T$	<u>69.0</u>	50.8
$C_E \subset C_I + \text{random perturbations}$	66.2	46.7

We do this by training the full iAmTime model, using all meta-training task-classes. We let $C_T =$ all domains other than {"Climate", "Healthcare"}, and $C_I =$ {"Climate", "Healthcare"} domains. The pre-training is done by sampling the pre-training datasets from domains C_T (Tables 7, 8).

The model is then evaluated on the forecasting-task by creating queries \mathcal{Q} from C_I in the benchmark datasets (see Tables 10, 9). For the $C_E \subset C_I$ variant, examples $\{\mathcal{E}_i\}_{i=1}^N$ are constructed by randomly selecting time-series from C_I . For

$C_E \subset C_T$, the examples are sampled from from C_T . For the third variant, the same $(Q, \{\mathcal{E}_i\}_{i=1}^N)$ pairs are used from the first variant. Then, perturbations are made on all the example time-series $\{\mathcal{E}_i\}_{i=1}^N$, by randomly applying one or more of the "Time-dependent transformation" functions discussed in Section 5.2.1.

Table 13 evaluates robustness to distribution shift during inference by varying the source of in-context examples provided to the model. When example demonstrations are drawn from the same unseen target-domain class set as the query ($C_E \subset C_T$), the model achieves the highest win rate, indicating that in-context examples effectively anchor the model to the test-time data distribution. When examples are instead drawn from the training-domain classes ($C_E \subset C_T$), performance degrades very slightly but remains strong, demonstrating that the model can still transfer learned forecasting strategies across domains through contextual adaptation. Introducing random perturbations to in-domain examples further reduces performance, confirming that the quality and distributional alignment of demonstrations directly influence the effectiveness of in-context task inference. These results suggest that the model uses in-context examples primarily as distributional and functional references rather than relying on memorized domain-specific parameters, enabling robust zero-shot generalization under *moderate* distribution shifts.

C.4. Example selection ablation

Table 14. CRPS scores of iAmTime compared with various baseline models on the multivariate data subset of GIFT-Eval benchmark. Models achieving the best and second-best scores are highlighted.

Dataset	<i>iAmTime</i>	<i>Chronos-2</i>	<i>TiReX</i>	<i>TimesFM-2.5</i>	<i>Toto 1.0</i>	<i>Moirai 2.0</i>	<i>Chronos-Bolt Base</i>	<i>TabPFN-TS</i>	<i>PatchTST</i>	<i>Seasonal Naive</i>
bitbrains_fast_storage/5T/long	0.667	0.703	0.672	0.831	<u>0.669</u>	0.807	0.748	0.885	0.669	1.177
bitbrains_fast_storage/5T/medium	0.647	0.623	0.638	0.766	<u>0.629</u>	0.694	0.755	0.949	0.642	1.198
bitbrains_fast_storage/5T/short	0.390	0.391	<u>0.380</u>	0.397	0.371	0.427	0.454	0.662	0.471	1.210
bitbrains_fast_storage/H/short	0.616	0.664	0.700	0.782	0.623	<u>0.615</u>	0.774	0.670	0.549	1.022
bitbrains_rnd/5T/long	0.568	0.873	0.632	0.743	0.589	<u>0.570</u>	0.756	0.819	0.664	1.175
bitbrains_rnd/5T/medium	0.678	1.005	<u>0.604</u>	0.846	0.628	0.596	0.605	0.819	0.620	1.169
bitbrains_rnd/5T/short	<u>0.401</u>	0.416	0.404	0.408	0.399	0.404	0.438	0.608	0.474	1.102
bitbrains_rnd/H/short	0.580	0.804	0.611	0.610	<u>0.593</u>	0.670	0.624	0.742	0.603	1.243
bizitobs_application/10S/long	0.049	0.045	0.052	0.053	<u>0.053</u>	0.056	0.109	0.049	0.054	<u>0.046</u>
bizitobs_application/10S/medium	0.025	<u>0.026</u>	0.038	0.033	0.034	0.037	0.104	0.041	0.047	0.043
bizitobs_application/10S/short	0.010	<u>0.010</u>	0.011	0.009	0.012	0.013	0.054	0.015	0.022	0.035
bizitobs_l2c/5T/long	0.237	0.298	<u>0.269</u>	0.279	0.533	0.300	0.738	0.306	0.324	0.648
bizitobs_l2c/5T/medium	0.254	<u>0.247</u>	0.251	0.241	0.316	0.261	0.445	0.261	0.332	0.520
bizitobs_l2c/5T/short	0.069	<u>0.069</u>	0.076	0.072	0.069	0.084	0.074	0.084	0.074	0.262
bizitobs_l2c/H/long	0.260	<u>0.267</u>	0.268	0.273	0.369	0.321	0.278	0.292	0.291	0.941
bizitobs_l2c/H/medium	0.209	<u>0.236</u>	0.252	0.237	0.356	0.274	0.254	0.237	0.263	0.904
bizitobs_l2c/H/short	0.167	<u>0.176</u>	0.212	0.179	0.199	0.235	0.189	0.210	0.217	0.521
bizitobs_service/10S/long	<u>0.051</u>	0.051	0.053	0.050	0.051	0.054	0.113	0.052	0.057	0.053
bizitobs_service/10S/medium	0.016	0.022	0.023	<u>0.018</u>	0.027	0.034	0.096	0.041	0.045	0.048
bizitobs_service/10S/short	0.011	0.010	0.012	<u>0.010</u>	0.011	0.014	0.051	0.019	0.025	0.040
ett1/15T/long	0.229	0.241	<u>0.234</u>	0.255	0.251	0.268	0.298	0.259	0.247	0.340
ett1/15T/medium	0.245	0.233	<u>0.237</u>	0.251	0.260	0.260	0.281	0.253	0.250	0.322
ett1/15T/short	0.158	0.165	0.161	0.157	0.162	0.160	<u>0.158</u>	0.167	0.191	0.241
ett1/D/short	0.283	0.274	<u>0.277</u>	0.300	0.284	0.287	0.287	0.298	0.304	0.408
ett1/H/long	0.258	0.275	0.281	0.288	<u>0.267</u>	0.323	0.311	0.295	0.297	0.471
ett1/H/medium	0.252	0.261	0.268	0.287	<u>0.254</u>	0.287	0.303	0.283	0.273	0.435
ett1/H/short	0.171	0.179	<u>0.176</u>	0.188	0.194	0.185	0.181	0.194	0.190	0.240
ett1/W/short	0.234	0.271	0.278	<u>0.241</u>	0.263	0.249	0.296	0.284	0.323	0.312
ett2/15T/long	0.090	0.093	0.092	0.097	0.088	0.102	0.111	0.101	0.098	0.133
ett2/15T/medium	<u>0.088</u>	0.087	0.089	0.094	0.093	0.098	0.110	0.100	0.094	0.124
ett2/15T/short	0.062	0.062	0.066	<u>0.063</u>	0.068	0.066	0.067	0.073	0.076	0.096
ett2/D/short	0.090	0.094	0.094	<u>0.092</u>	0.111	0.093	0.094	0.126	0.131	0.153
ett2/H/long	<u>0.103</u>	0.105	0.114	0.101	0.108	0.109	0.117	0.139	0.130	0.208
ett2/H/medium	0.103	0.109	0.107	0.101	<u>0.102</u>	0.111	0.115	0.121	0.125	0.186
ett2/H/short	0.064	0.064	<u>0.064</u>	0.064	0.065	0.064	0.063	0.073	0.074	0.089
ett2/W/short	0.093	0.090	<u>0.087</u>	0.087	0.106	0.085	0.088	0.099	0.142	0.134
jena_weather/10T/long	0.048	0.051	<u>0.049</u>	0.050	0.050	0.060	0.064	0.053	0.066	0.237
jena_weather/10T/medium	0.048	0.050	<u>0.048</u>	0.049	<u>0.049</u>	0.059	0.057	0.054	0.065	0.212
jena_weather/10T/short	0.025	0.030	0.027	0.028	<u>0.027</u>	0.036	0.033	0.034	0.064	0.155
jena_weather/D/short	0.043	0.047	0.044	0.045	0.051	<u>0.043</u>	0.045	0.047	0.053	0.211
jena_weather/H/long	<u>0.056</u>	0.059	0.059	0.055	0.057	0.058	0.062	0.103	0.076	0.419
jena_weather/H/medium	0.050	<u>0.050</u>	0.053	0.051	0.053	0.055	0.054	0.058	0.069	0.343
jena_weather/H/short	0.040	0.042	<u>0.041</u>	0.043	0.042	0.042	0.042	0.042	0.050	0.154